The Ediacaran-Cambrian transition in the Cantabrian Zone (North Spain): sub-Cambrian weathering, K-metasomatism and provenance of detrital series

J.M. Ugidos,[a*] P. Barba,[a] M.I. Valladares,[a] M. Suárez,[a] R.M. Ellam, [b]

a *Departamento de Geología, Facultad de Ciencias, Universidad de Salamanca, 37008 Salamanca, Spain*

b *Scottish Universities Environmental Research Centre, East Kilbride G75 OQF, UK*

Abstract: The Upper Ediacaran detrital succession in the Cantabrian Zone shows geochemical and mineralogical changes resulting from sub-Cambrian weathering during the Late Ediacaran worldwide sea-level fall. Relative to the unaltered rocks the altered ones show crosscutting rubefaction of varying thickness a remarkable increase in illite, K_2O, Rb and Cs indicating K-metasomatism, and also depletion in MgO, CaO, Na_2O, Be and Sr, but not in Zr, Nb, Y, Sc. The basal Cambrian siliciclastic rocks mostly consist of detritus derived from the Ediacaran materials, as demonstrated by the geochemical and Nd-isotope data [$\varepsilon_{Nd}(t)$ ranges: -3.4 to -2.1, and -3.6 to -1.8, respectively)]. However, these geochemical features of the basal Cambrian change upwards to more evolved compositions with lower $\varepsilon_{Nd}(t)$ values (-4.9 to -5.8). This change is the same as coinciding with the Ediacaran-Cambrian unconformity in the Central Iberian Zone and the Ediacaran siliclastic rocks of this zone and their unaltered equivalents of the Cantabrian Zone share the same geochemical features. This geochemical homogeneity rules out a significant coeval juvenile contribution to the Upper Ediacaran series. Thus, the juvenile supply took place in a geological setting different from the one where the Ediacaran series were finally deposited.

Supplementary material: [sampling, sample location, analytical techniques, diffractograms, tables of analyses, and figures] is available at.

Worldwide, the Ediacaran-Cambrian boundary corresponds to a major unconformity in most sections, suggesting a possible eustatic fall in sea level (Bartley *et al.* 1998; Saylor 2003; Knoll *et al.* 2004; Pyle *et al.* 2004). The duration and magnitude of this unconformity vary between sections but its age appears to be the same within the precision afforded by biostratigraphic and chemostratigraphic correlations. Reflecting this sea-level fall, the Late Ediacaran-Early Cambrian interval is characterised by elevated chemical weathering rates, as suggested by the steep rise in the normalised seawater strontium isotope curve (Shields 2007). Sub-Cambrian weathering profiles developed in many areas of Gondwana after the Pan-African orogeny on the Precambrian basement at continental scale (Avigad *et al.* 2005; Avigad & Gvirtzman 2009; Johnson *et al.* 2011; Sandler *et al.* 2012 and references therein) and the age of this weathering (542.62 ± 0.38 Ma, Parnell *et al.* 2014 and references therein) is close to that of the Ediacaran-Cambrian boundary (541 ± 0.13 Ma, Bowring *et al.* 2007). Also, the Upper Ediacaran normal faulting and associated alkaline magmatism indicate a within-plate extensional tectonic setting in the northern margin of the West African craton (Ennih & Liégeois 2001; Piqué 2003; Thomas *et al.* 2004; Soulaimani *et al.* 2004; Álvaro *et al.* 2010).

In the Cantabrian Zone (Fig. 1), the Upper Ediacaran series were deposited by turbidity currents (Pérez Estaún 1978) and show weathering and rubefaction below the Precambrian-Cambrian boundary (van der Bosch 1969; Gutiérrez-Alonso *et al.* 2004), which is an angular unconformity. In the Central Iberian Zone (Fig. 1A) the Ediacaran-Cambrian boundary is a disconformity, expressed as an irregular and strongly erosional surface related to a worldwide eustatic fall in sea level. A study of facies and facies associations of the Upper Ediacaran and Lower Cambrian detrital series revealed that the sedimentation resulted predominantly from gravity flows, such as turbidity currents and debris flows in slope and base-of-slope environments (Valladares *et al.* 2000, 2006) while in the Cantabrian Zone the setting of the basal part of the Lower Cambrian succession was a continental environment (Aramburu *et al.* 1992; Rubio-Ordoñez *et al.* 2004). The aims of the present work are two-fold: to study the processes during the Ediacaran-Cambrian transition in the Cantabrian Zone and to determine the provenance of the Upper Ediacaran and Lower Cambrian detrital series. The results strongly suggest that the Upper Ediacaran detrital rocks derived from the same source as that of the equivalent rocks in the Central Iberian Zone while the Lower Cambrian siliciclastic rocks derived from mixtures of the unaltered and rubefacted Ediacaran materials. The contribution of an older crustal component increases upwards.

Geological setting

The Ediacaran rocks, known as the Narcea schists group (Fig. 2) or Mora formation, outcrop in the east part of the Narcea antiform (Fig. 1B), within the Cantabrian Zone, and its western boundary (Fig. 1B) is La Espina thrust (Pérez Estaún *et al.* 1990). In these rocks Pérez Estaún (1978) differentiated 1500-1700 m of alternating greywackes and shales with abundant sedimentary structures of turbiditic origin. The age of the Narcea schists is constrained by the presence of the acritarchs *Sphaerocongregus variabilis* and *Palaeogomphosphaeria caurensis* (Martín Parra *et al.* 1989; Palacios & Vidal 1992), both regarded as indicative of a late Vendian age (Vidal *et al.* 1994). Detrital zircons from the sandstones of the Narcea schists provided an age of 553±4 Ma (Fernández-Suaréz *et al.* 2014), which indicates a younger age for the Narcea succession in the Cantabrian Zone. The Upper Ediacaran series show weathering and crosscutting rubefaction up to 25 m thick below the Precambrian-Cambrian boundary (van der Bosch 1969).

In the Cantabrian and Central Iberian zones the Ediacaran siliciclastic successions were deposited predominantly from debris flows and turbidity currents in slope, base-of-slope and deep sea fan environments (Pérez Estaún 1978; Valladares *et al.* 2000). However, in the outcrops of the eastern-most area of the Central Iberian Zone, Montes de Toledo, and also in the Iberian Ranges (Fig. 1A, MT and IR, respectively), the upper part of the respective Edicaran successions (Ibor and Paracuellos groups, Fig. 2) are mixed platforms (siliciclastic-carbonate), from offshore to shoreface, with sandy and ooidal-bioclastic shoals (Álvarez Nava *et al.* 1988; Calvet & Salas 1988; Álvaro & Blanc-Valleron 2002; Álvaro *et al.* 2008). The presence of the ichnospecies *Torrowangea roseis* (Liñán & Tejero 1988) and *Cloudina*-like shelly fossils (Álvaro & Blanc-Valleron 2002) in the Paracuellos group (Fig. 2), together with the presence *in situ* of skeletal fossil *Cloudina* in the platform carbonates of the Ibor group, indicates a latest Ediacaran age for the both groups (Vidal *et al.* 1994). In the Domo de las Hurdes (Fig. 1A, DH), this upper part of the Ediacaran succession exhibits laminated black shales with an intercalation of alternations of limestone breccias and stratified sandstone± limestone couplets (Unit IV. Valladares *et al.* 2000), which were deposited from debris flows and turbidity currents in a mixed slope apron (Valladares 1995). In the Cantabrian Zone and IR, the basal Lower Cambrian detrital series were deposited in continental environments (Aramburu *et al.* 1992; Rubio-Ordóñez *et al.* 2004; Álvaro *et* *al.* 2008), while in the Central Iberian Zone the equivalent series were mainly deposited in slope and base-of-slope environments (Valladares et *al.* 2000).

The Herrería group (Fig. 2) predominantly consists of sandstones with some levels of conglomerates, shales and carbonates, with a thickness varying between 900 m in Barrios de Luna (Fig. 1B) and 1500 m in the Cangas de Narcea-Mieldes areas (Comte 1959). The lower part of this group consists of conglomerates that locally displays volcanic clasts, and have a lenticular geometry (Fig. 1B), interpreted as a large deposition cone (Parga & Luque 1971). Palaeontological data have revealed two fossil assemblages that begin with the record of *Phycodes* (=*Treptichnus*) *pedum* 4 m above the angular unconformity of the base of the Herrería group (Palacios & Vidal 1992), followed by *Rusophycus* and *Cruziana* species, indicating that this member yielded associations of ichnofossils suggestive of a Late Corduban age (Liñan *et al.* 2002).

The Lower Cambrian begins with conglomerate and sandstone-shale alternations deposited in alluvial and braided-channel environments at the base, which evolved upwards to tidal environments. In a restricted area close to Mieldes **(**Fig. 1B**)** this conglomerate has completely rubefacted angular clasts of shales, and well-rounded quartzite and volcanic clasts of undeformed pyroclastic rocks, mostly rhyolites and dacites with sericitised K-feldspar, displaying a coating of rubefaction (Rubio-Ordóñez *et al.* 2004, 2015). Some of these volcanic clasts contain zircons whose morphology is typical of zircons observed in alkaline magmas (Rubio-Ordóñez *et al.* 2006; Rubio-Ordóñez 2010). The latter authors suggested a change in the tectonic conditions from compressive to extensional at the end of the Ediacaran to explain this alkaline volcanism. However, the volcanic clasts were intensely affected by hydrothermal processes that did not affect the other components of the conglomerate, and the geochemical data do not represent the original magmatic composition (Rubio-Ordóñez 2010; Rubio-Ordóñez *et al.* 2015). In the rest of the Cantabrian Zone, at the sites where the base of the Herrería group outcrops the conglomerates lack volcanic clasts, and well-rounded clasts of white quartz prevail. The source area of the Lower Cambrian detrital series was to the east of the present location of the Cantabrian Zone (Aramburu *et al.* 1992 and references therein) but post-Cambrian sediments cover this area, and no other Ediacaran outcrops are observable. In the IR and Sierra de la Demanda (Fig. 1A, SD), the basal Lower Cambrian also has conglomerate beds but no volcanic clasts have been reported; instead, subrounded clasts of white quartz prevail (Álvaro *et al.* 2008; Ábalos *et al.* 2011).

Mineralogy

XRD semi-quantitative data on the rock-forming minerals in the rubefacted and unaltered Ediacaran and the Cambrian shales reveal that albite and chlorite are relatively abundant only in the Ediacaran shales but albite is absent in the equivalent rubefacted and Cambrian shales while chlorite has varying but lower contents in these two groups of shales than in the Ediacaran ones (Table 1). Some samples have hematite (≤ 5%), this mineral being more abundant in the rubefacted shales, and only samples BEL-2 and BEL-9, both corresponding to the Cambrian, contain K-feldspar (12% and 4%, respectively). The Cambrian samples can be separated into two sub-groups: those having heterogeneous mineral contents and those with homogeneous contents (labels: BEL-2, 9 and LR-3, and BEL-3, PS-2, and 6, respectively) that correspond to different positions in the stratigraphic series (see below). Figure 3 shows the enrichment in illite and depletion in chlorite of the Ediacaran rubefacted shales relative to the unaltered ones, together with the overlapping plot of the rubefacted and Cambrian shales.

Stratigraphy

Nearly 2700 m of stratigraphic logs from five partial sections of the Ediacaran succession (Narcea group) in the Cantabrian Zone were studied. This succession is several hundred metres thick and consists of siliciclastic rocks, predominantly sandstones and shales, and less abundant paraconglomerates, of Late Ediacaran age. The lithological uniformity in all partial sections hindered the division of this succession into lithostratigraphic units. These lithologies form two types of sequence. The predominant one is a thinning- and fining-upward sequence, 8 to 12 m thick and occasionally up to 30 m, from paraconglomerates to shales that are interpreted as a channel-fills deposited by different sediment gravity flows (e.g. debris flows and high- and low-concentration turbidity currents) and vertical settling from the suspension cloud of the turbidity currents. The frequent presence of a more or less thick lag over a basal erosive surface is interpreted as a channel lag deposit and indicates that its deposition could be coeval with the period of maximum activity in the channel and agradation of the levees due to overflow of the finer sediments before their silting (Torres *et al*. 1997).

The other type consists of thickening- and coarsening-upward sequences, generally 0.7 to 5 m thick. From bottom to top, these sequences have basal shales, followed by alternations of sandstone-shale and massive sandstones at the top. This facies association corresponds to lobe deposits. However, in the present case this type of sequences is scarce, and is associated with fine-grained facies (shales and sandstone-shale alternations) and hence interpreted as overbank deposits formed in interchannels areas adjacent to the channels during their filling phases as small lobes in the inner deep-sea fans.

In general, according to the classification of Folk (1980), the Ediacaran sandstones of the Cantabrian Zone are medium-grained litharenites consisting mostly of moderately- to poorly-sorted grains of angular quartz (35-43%), chert (19-35%), the clasts of black shales, sandstones and feldspars being less abundant (< 15%) and isolated (< 1%) microclasts of igneous groundmass consisting of plagioclase laths and quartz.

More than 800 m of stratigraphic logs from five partial sections of the basal 200 m of the Lower Cambrian succession of the Herrería group were studied. This succession consists predominantly of siliciclastic rocks, shales being more abundant in the area of Vega de los Caballeros (Fig. 1B), where the Herrería group has a carbonate level about 30 m thick displaying a lenticular geometry at about 40-50 m above its base. Contrastingly, in the area of Mieldes-Parada la Vieja (Fig. 1B) conglomerates and sandstones predominate, and the carbonate level has not been identified.

Figure 4 shows two stratigraphic logs having and lacking, respectively, the carbonate level. In both sections, three intervals were distinguished. The lower one is 40 m thick and its lower boundary is an erosive surface in both logs. At Parada la Vieja, overlying this surface there are fining- and thinning-upward sequences that begin with paraconglomerates with a red sandy matrix and clasts of white quartzite, and rubefacted and black shales, followed by very coarse- and coarse-grained red sandstones, finishing with red shales (Fig. 4). The clasts are disorganised and are sometimes vertical (debris flows), and occasionally there is inverse grading and horizons of clasts parallel to the stratification within the sandstones. At Vega de los Caballeros this lower interval begins with a thin level of microconglomerate with clasts of rounded white quartzite. The rest of the interval consists of green shales with some thin levels of coarse- and medium-grained sandstones with clasts of green shales, and lenses of fine-grained sandstones with a ripple lamination.

The middle interval is carbonated at Vega de los Caballeros. It consists of recrystalised sandy limestones forming coarsening- and thickening-upward sequences between 1.5 and 2.7 m thick (Fig. 4) that sometimes finish with ferruginous crusts and that can be interpreted as oolithic and bioclastic shoals in an inner high energy platform, with the possible emersion of the tops of some shoals. At Parada la Vieja, this middle interval is formed by siliciclastic thickening-upward sequences 2 to 3 m thick consisting of coarse-grained sandstones with a planar cross stratification that alternate with green shales. The sandstones show herring-bone and sigmoidal stratifications. All these sedimentological features can be interpreted as tidal shoals that have migrated in the present SE-NW direction (130º and more scarce to 300º) according to the paleocurrents (Fig. 4). Towards the top of the interval, these sequences alternate with fining-upward sequences 1.5 to 3.5 m thick, with a basal erosive surface, overlaid by microconglomerates with a normal grading and sandstones with trough and planar cross stratification, and the sequences finish with green shales. These sequences are interpreted as tidal channels that would have transported the sediments from the present NE to the SW (230º) according to the paleocurrents crossing the tidal shoals (Fig. 4). In this middle interval, there are frequent flaser, wavy and lenticular stratifications. All these features indicate a subtidal environment in an inner platform.

Finally, the upper interval is siliciclastic in both logs (Fig. 4). At Parada la Vieja, this interval is similar to the lower one, coarse-grained sandstones and conglomerates predominating in thickening- and coarsening-upward sequences of 2 to 7 m thick in the lower part, while the uppermost metres are thinning- and fining-upward sequences with an erosive basal surface. The conglomerates have clasts of up to 4 cm of white quartzite and red shales. The sequences are interpreted as bars and channels deposited in a fluvial environment. At Vega de los Caballeros it is possible to distinguish a lower part that is 65 m thick in which grey shales with scarce lenticular fine-grained sandstones with linguoid ripples and middle- to fine-grained sandstones prevail in fining-upward sequences of 1 m thick overlying an erosive base. In the upper 20 m of the section, shales are rare except at the top, where they are red, although coarse- and middle-grained sandstones with erosive base and channel geometry predominate. As at the Parada la Vieja, this upper part corresponds to a fluvial environment, while the pelitic lower part is interpreted as a low-energy marine environment with predominant settling.

Geochemistry

Ediacaran shales and sandstones

Contents of alkaline and alkaline earth elements and their ratios do not show significant differences in the Ediacaran shales or in the sandstones. The shales show rough negative covariation in SiO_2-major element diagrams only for Al_2O_3 and Fe_2O_3. Also, TiO_2-P_2O_5, and TiO_2-Zr diagrams define positive correlations for shales (r^2 = 0.75 and 0.77, respectively; n = 20) suggesting homogeneous proportions of Ti-minerals, phosphates and zircon in these rocks. The Sc contents in the sandstones are relatively high and show rough positive covariations with TiO_2, Yb and Y. Sc may be stored in Ti- and Fe- and rare earth element (REE)- minerals (Schock 1975). Thus, a plausible interpretation of the relatively high Sc contents in the sandstones and these covariations is that recycling and sorting favoured accumulation of heavy minerals storing Sc. The shales also show these covariations. The shales and sandstones exhibit parallel REE patterns (Fig. 5a,b) and the Ediacaran shales from Cantabrian Zone and NIBAS (Neoproterozoic Iberian Average Shale. Ugidos *et al.* 2010) show the same mean REE patterns and those of the corresponding mean sandstones (Ugidos *et al.* 1997b) are also the same (Fig. 5c). Normalised to the composition of the upper continental crust (UCC, Rudnick & Gao 2005; Hu & Gao 2008), the mean shales of the Cantabrian Zone and NIBAS define the same multielement patterns and also the two corresponding mean sandstones (Fig. 5d). All these rocks exhibit a strong depletion in Sr, and the sandstones show enrichment in Zr with respect to the shales.

Sub-Cambrian alteration and K-metasomatism of the Ediacaran rocks

The abundances of SiO_2, TiO_2, Al_2O_3 and Fe_2O_3 in the rubefacted shales lack relevant changes that could be interpreted as being related to oxide gain or loss with respect to those of the unaltered ones. However, the abundances of other oxides and elements such as MgO, CaO, Na_2O, P_2O_5, Be and Sr are lower, and those of K_2O, Rb, Cs, and Ge are higher in the rubefacted rocks. To quantify these differences, the model compositional changes (MCC) of element concentrations in the rubefacted shales were calculated with respect to the unaltered ones by using the expression: MCC = $[(E_{G1}-E_{G2})/E_{G2}]*100$ (Páez *et al.* 2010), in which E_{G1} and E_{G2} are the median and mean element concentrations in the group of the rubefacted and unaltered rocks respectively (Table 2). The abundances of some oxides such as CaO and Na_2O are below the detection limit in many rubefacted shales. Thus, the parameters involving these oxides were calculated accepting the values of the detection limits (0.1% and 0.05%, respectively) as the maximum contents.

Although in Table 2 there are some differences in the results depending on whether the calculations were made using the median or the mean values of element contents (e.g., Sc enrichment is 10.9% or 3.2% in the rubefacted shales depending on whether the median or the mean abundance is used; similarly, the Cs enrichment is 226% or 166%), in general there is good agreement between both groups of calculations. The major differences are probably a consequence of the relatively low number of analyses and ranges of some element contents with no or scarce intermediate values. Thus, the median values of some elements are strongly dependent on the number of data in each extreme group of values, and hence the compositional change can be exaggerated (either higher or lower) when the mean and median differ substantially. To minimise this effect, any change, depletion or enrichment of an element is accepted only if the results from the both calculations are comparable.

The strong depletion of MgO, CaO, and Na_2O, and the strong increase in K_2O contents are consistent with the trend parallel to the chlorite-illite join defined by the Ediacaran unaltered and rubefacted shales (Fig. 3). The Rb and Cs contents of the rubefacted ones increase remarkably, probably incorporated to illite (McLennan *et al.* 1990), and those of Be and Sr decrease due to leaching during weathering. Although some samples of the rubefacted shales have lower REE contents, most of their REE patterns (Fig. 5e) overlap those of the unaltered ones and it is unclear whether the calculated loss of REE really occurred or whether it might be due to the low number of samples. Whatever, the possible loss of REE did not cause significant Sm-Nd fractionation given that the unaltered (0.194-0.211; mean = 0.203; st. dev. = 0.01) and rubefacted shales (0.197-0.220; mean = 0.209; st. dev. 0.01) have almost identical Sm/Nd. Furthermore, the Nd-isotope results also suggest that Sm/Nd was not affected by weathering (see below). Y, Zr, V, Nb, Ta, and Cr (not included in Table 2) do not show significant changes. A loss of U occurred probably due to the oxidation of U^{+4} to the more soluble U^{+6} (McLennan *et al.* 1993), and also of Th (Table 2) as is suggested by the lower mean Th/Sc ratio of the rubefacted shales (Table 3). Probably, acidic waters resulting from sulphide oxidation (S content in six shales: 0.01 to 0.9%, unpublished data) during weathering affected the Ediacaran shales, favoured the precipitation of hematite, released elements such as Co, Ni, Cu, Zn, Pb, and As, and also favoured the dissolution of phosphates and the release of REE, Th and U, and the desorption of Be from clays (Grew 2002; Ryan 2002; Harlavan *et al.* 2009; Åström *et al.* 2010). Germanium is an element sequestered by secondary clays during weathering (Scribner *et al.* 2006) and its content is increased by about 20% in the rubefacted shales (Table 2).

The rubefacted shales are the only ones that show loss of Ca and Na, and a remarkable increase in K. This suggests a process of K-metasomatism related to weathering and rubefaction. A process of K-metasomatism may have different causes and affect siliciclastic and volcanic rocks, but in all cases the source of K is local rather than from externally derived fluids, as demonstrated by Hutcheon *et al.* (1998). In general, K-metasomatism is associated with extensional crustal settings and increases the illite contents in the siliciclastic rocks affected, causes Rb enrichment, and Ca, Na, Mg and Mn depletion (Beratan 1999; Ennis *et al.* 2000; Páez *et al.* 2010), as occurred in the area studied. Low-temperature K-rich brines resulting from the evaporation of marine waters in restricted environments and the percolation of basinal fluids have been proposed as causes of metasomatising processes (Munz *et al.* 1995; Leising *et al.* 1995; Ennis *et al.* 2000; Sandler & Harlavan 2006). Thus, it is possible that during the Upper Ediacaran sea-level fall marine water might have remained isolated in coastal environments and evolved to K-rich brines, which could have resulted in the K-metasomatism and rubefaction of the Ediacaran rocks of the Cantabrian Zone during the intense worldwide weathering processes in sub-Cambrian times.

Cambrian shales

Two groups of Cambrian shales can be established (see also Table 1): those underlying and those overlying the carbonate level, referred to below as the underlying and overlying shales, respectively. The underlying and rubefacted shales show similar ranges of SiO_2 contents; they lack or have minor contents of MnO, CaO and Na_2O; they have relatively high contents of K_2O, Rb, Cs and Ge, and most of the mean element ratios of both groups of shales are the same (Table 3). The rubefacted shales have the same Zr/Nb ratios as their parent rocks but increased Rb/Zr ratios that overlap those of the Cambrian shales (Fig. 6). These geochemical similarities, together with the presence of angular clasts of the rubefacted shales in the basal Cambrian conglomerate, reflect the contribution of the Ediacaran rocks to the Cambrian series. However, the underlying shales also have higher contents of Al_2O_3, K_2O, REE and Th, and lower Fe_2O_3 and MgO, and higher K_2O/Al_2O_3 ratios than the Ediacaran shales. The only major element covariations defined by the underlying shales are SiO_2-Al_2O_3, SiO_2-K_2O and Al_2O_3-K_2O (r^2 = 0.98, 0.92 and 0.95, respectively; n = 5). These results together, strongly support the notion that the increase in Al_2O_3 and K_2O contents, and in the K_2O/Al_2O_3 ratio (range: 0.353-0.386) is due to the relative increase in detrital illite derived from K-metasomatised and weathered Ediacaran rocks, although it is also possible that this high ratio may be partially due to the presence of undetected quantities of K-feldspar. The lower Fe_2O_3 and MgO contents of the underlying shales are probably related to the illitisation of the chlorite of the rubefacted shales (Fig. 3), the leaching of Mg and a redistribution and loss of hematite during the sub-Cambrian weathering and erosion. The underlying shales also have higher contents of Be, REE and Th and a lower Eu/Eu* ratio than the rubefacted ones probably due to the contribution of the Ediacaran weathered igneous rocks.

The overlying shales are characterised by lower contents of SiO_2 and higher contents of the other major elements, and higher Eu/Eu* and $(La/Yb)_N$ ratios, but also lower contents of Rb, Cs and Zr. Mean element ratios such as Al_2O_3/TiO_2, Ti/Nb, Th/Sc and Zr/Hf and others in Table 3 are the same in both groups of shales. Thus, the underlying and overlying shales share some geochemical features while other features, such as the lower contents of Rb, Cs and Zr, the higher contents of light REE and the relatively low Rb/Sr, Cs/Be and Zr/Nb ratios (Table 3) in the overlying shales, indicate a decreasing proportion of detritus from the rubefacted rocks and an increasing contribution of a new component that also supplied K-feldspar to these shales (Table 1). Plausibly, the higher Eu/Eu* ratio of the overlying shales could be due to the presence of K-feldspar and the higher $(La/Yb)_N$ ratio could be related to a higher content of light REE and lower content of zircon, as suggested by the lower Zr of these shales.

Nd isotopes

The data in Table 4 strongly suggest a higher proportion of juvenile material in the Ediacaran and in the above-mentioned underlying shales than in the overlying ones. The $\varepsilon_{Nd}(t)$-$f_{Sm/Nd}$ diagram has the potential to identify mixtures of detritus derived from upper-crustal rocks and juvenile contributions coeval with sedimentation which would define sub-horizontal to diagonal trends. Actually, the shales show little evidence of correlation in the $\varepsilon_{Nd}(541)$-$f_{Sm/Nd}$ diagram (Fig. 7a) approaching vertical arrays. Redistribution of REE could result in vertical arrays (Bock *et al.* 1994) but the range of $^{147}Sm/^{144}Nd$ (Table 4) within the various groups of shales, even the rubefacted ones, are narrow suggesting that no substantial fractionation of REE affected these rocks during exogenic processes (Jahn & Condie, 1995).

Discussion and conclusions

Provenance of the Ediacaran and Cambrian detrital series of the Cantabrian Zone: major and trace elements and Nd-isotope results

Mafic rocks contributing to siliciclastic sediments increase the contents of Sc, Cr and plagioclase while those of La and Th increase if the source rocks are felsic (Condie & Wronkiewciz, 1990; Eriksson *et al.* 1992; Crichton & Condie, 1993; McLennan *et al.* 1993, 1995, 2006; Feng *et al.* 1993; Cox *et al.* 1995). According to these authors, the abundance of volcanic lithic fragments in sandstones, the relatively low values of La/Sc, La/Cr, Th/Cr and Th/Sc, and the high Eu/Eu* ratios are expected in fine-grained siliciclastic rocks resulting directly from active margins and related settings, and considerable petrological and geochemical variability is also expected. By contrast, the homogeneity reflects the recycling and buffering of mixtures of different sources (Garrels, 1988; McLennan, 1989; Cullers, 1994; Brown *et al.* 2003; McLennan *et al.* 2006). Moreover, sedimentary recycling causes an enrichment of Zr abundance in sandstones relative to contents in related fine-grained sediments, while there are no systematic differences in the sediments of active tectonic settings (McLennan *et al.* 1990). Also, relatively high K_2O/Na_2O and Rb/Sr ratios, and high CIA (Nesbitt & Young, 1982) values are expected for shales (McLennan *et al.* 1990, 1993). Another useful diagram, Th/Sc-ε_{Nd}(t), relates the composition of the sediments to the mean provenance age (McLennan *et al.* 1993) and potentially reflects the contribution of felsic or mafic components to detrital rocks.

The Ediacaran shales studied have relatively high K_2O/Na_2O (1.24-2.81) and Rb/Sr (0.85-2.49) ratios and CIA values (65.10-73.16). The sandstones are enriched in Zr (mean: 257, range, 196-321, s.d. 44) with respect to the shales (197, 174-231, s.d. 16). The Eu/Eu* ratios of the 80% of shales are lower than 0.70 and their mean Eu/Eu* ratio (0.67) is lower than those of the UCC (Table 3). The Ediacaran shales of the Cantabrian Zone and NIBAS share element ratios (Table 3) regardless of whether such ratios (e.g., Al_2O_3/TiO_2, Ti/Zr, La/Sc, Zr/Sc, Zr/Nb, and Th/Nb) are dependent upon mineral proportions, or on diagenesis or other processes that could affect mobile/immobile element ratios (e.g., Rb/Th and Rb/Zr). Furthermore, the element ratios such as La/Cr, La/Sc and Th/Sc among others used as provenance indicators, are the same as those of the UCC (Table 3). The two mean sandstones also share most trace element ratios and both the shales and sandstones have the same mean Ti/Nb, La/Cr, Cr/Th and Th/Nb ratios (Table 3). The Ediacaran and Cambrian shales show little evidence of correlation in the $\varepsilon_{Nd}(541)$-$f_{Sm/Nd}$ and Th/Sc-$\varepsilon_{Nd}(541)$ diagrams (Fig. 7a, b). Also, the $\varepsilon_{Nd}(541)$ values of the Ediacaran shales presented here and those from the Central Iberian Zone (-3.8 to -1.8, Tassinari *et al.* 1996; Ugidos *et al.* 1997a, 2008, recalculated to 541Ma) are the same. Therefore, the Ediacaran detrital rocks have a remarkable geochemical homogeneity in these zones.

The geochemical uniformity is not compatible with a widespread volcanism coeval with the sedimentation of detrital successions and none of the criteria described above used to define a coeval contribution of magmatic arcs to detrital sediments are fulfilled by the Ediacaran detrital series studied here. Therefore, these series derived from recycled and homogenised mixtures of different materials. However, the relatively high $\varepsilon_{Nd}(541)$ of the Ediacaran shales requires a juvenile contribution to these detrital sediments. Thus, it is concluded that this juvenile contribution occurred in a geological setting different from the one in which the Ediacaran series were finally deposited after the recycling and homogenisation of all the components. An inmature passive margin is the most plausible setting for the basin of the Ediacaran detrital series.

The Cambrian series: inheritance from the Ediacaran detrital and volcanic rocks

The Cambrian conglomerate overlying the Ediacaran-Cambrian angular unconformity has completely rubefacted angular clasts of shales and well-rounded volcanic clasts displaying a coating of rubefaction. The sources of these materials were the Ediacaran series and volcanic rocks affected by the worldwide weathering process in Late Ediacaran times (542.62 ± 0.38 Ma, Parnell *et al.* 2014). The volcanic clasts in the Cambrian conglomerate have been found in a relatively restricted area close to Mieldes (Fig. 1), but no volcanic rocks have been found in the Ediacaran successions of the Cantabrian Zone or in the other basal Cambrian conglomerates of the region studied in this work. Also, in the IR and SD (Fig. 1) the Ediacaran successions lack igneous rocks, and no volcanic clasts from the basal Cambrian conglomerates have been reported (Álvaro *et al.* 2008; Ábalos *et al.* 2011, 2012). It may be inferred that the volcanic clasts in the basal conglomerate of the Cantabrian Zone resulted from volcanic activity of local importance, probably related to extensional faults in the Late Ediacaran.

Based on the observations presented here, the basal Cambrian series mostly consist of detritus derived from the Ediacaran rocks underlying the angular unconformity but the shales overlying the carbonate level also received a significant contribution of a component that supplied K-feldspar and increased the abundances of LREE and lowered the $\varepsilon_{Nd}(541)$ values. Therefore, the contribution of the inherited Ediacaran detritus to these shales decreased and the proportion of more evolved detrital components increased. Two main possibilities, perhaps coeval, could explain the geochemical change: a) The rise in sea-level gradually covered the outcropping Ediacaran rocks, which would have decreased their contribution to the Cambrian sediments; b) A decrease in the relative extension of Ediacaran rocks at the source due to erosion and peneplanation and an increase in subaereal exposures of more evolved compositions.

The Cambrian shales of the IR exhibit an increase in the mean contents of illite (from 39 to 59%) and K_2O (4.0 to 5.6%) and a decrease in the mean contents of chlorite (15 to 5%) and feldspar (16 to 5%), CaO (1.0 to 0.6%) and Na_2O (1.9 to 0.4%) with respect to those of the Upper Neoproterozoic (Table 1, in Bauluz *et al.* 2000). Furthermore, the same geochemical parameters that discriminate the Ediacaran from Cambrian shales in the Central Iberian Zone also separate the equivalent shales in the IR (Valladares et *al.* 2002b).

Paleogeography

On the basis of the previous data mentioned in Geological Setting and of the stratigraphic data reported in this study, it is suggested that the upper part of the Ediacaran successions (Paracuellos and Ibor groups, Fig. 2) eastwards of the Iberian Massif (IR and MT, Fig.1) were deposited in a platform environment (Calvet & Salas, 1988; Álvaro & Blanc-Valleron, 2002; Álvaro *et al.* 2008) while in the rest of the Central Iberian Zone the upper part of the Ediacaran succession (unit IV, Fig. 2) was deposited in slope and base-of-slope environment (Valladares *et al.* 2000) during Late Ediacaran times. However, in the Cantabrian Zone the Ediacaran succession was deposited in deep-sea fans (Pérez Estaún, 1978; this work) but geological processes such as extensional tectonics, differential block subsidence, and the development of high-relief areas favoured the erosion of the materials equivalent to those of Paracuellos and Ibor groups and the Unit IV, which have carbonate beds and *Cloudina*. Thus, these beds are absent in the Narcea succession although the remaining part is also of Late Ediacaran age (< 553 Ma). Therefore, it is unclear whether a shallow or a deep environment was present in the Cantabrian Zone in the latest Ediacaran times. In the Cantabrian Zone and IR, the basal detrital successions of the Herrería group and Bámbola formation (Fig. 2) were respectively deposited on alluvial plain sequences and braided channel environments (Aramburu *et al.* 1992; Rubio-Ordoñéz *et al.* 2004; Álvaro *et al.* 2008) during the Early Cambrian, while the basal Cambrian succession in the Central Iberian Zone was mostly deposited in slope and base-of-slope environments (Valladares *et al.* 2000). Therefore, the source area of the Iberian basin was placed at the present ENE in the Late Ediacaran. During the Early Cambrian, the continental environments were also towards the present ENE and the deep basin towards SW. In the both cases the source area of the Iberian basin would have been located at the present NE.

Geological processes around the time of the Ediacaran-Cambrian boundary

According to the data presented here, the sequence of geological processes in the Cantabrian Zone close to the Ediacaran-Cambrian boundary is synthesised in Fig. 8 as follows:

a) The Narcea group was deposited in channels and small lobes in the interchannel areas of the inner deep-sea fans. This group is younger than 553 ± 4 Ma (age of the youngest detrital zircons, Fernández Suárez *et al.* 2014).

b) After the sedimentation of the Narcea group and before the sub-Cambrian weathering (542.62 ± 0.38 Ma, Parnell *et al.* 2014), extensional tectonics and volcanism associated with related faults occurred. The morphological types of the zircons in the volcanic clasts from the basal Cambrian are typical of alkaline magmas (Rubio-Ordóñez *et al.* 2006). Thus, the general geological setting is similar to that seen in the northern margin of Gondwana (see above).

c) The extensional regime resulted in differential block subsidence and high-relief areas (Valladares *et al.* 2002a; Rubio-Ordóñez *et al.* 2015). Then, the erosion of the Ediacaran materials began, and probably initiated the sea-level fall around the Ediacaran-Cambrian boundary, followed by the sub-Cambrian weathering of the Ediacaran rocks (Fig. 8).

d) During the sea-level fall weathering would have caused rubefaction and the K-rich brines resulting from the evaporation of marine water in restricted environments would have percolated and caused K-metasomatism of the Ediacaran rocks. The sub-Cambrian erosion would have favoured peneplanation and transport, and the rolling of volcanic clasts that favoured generation of their rubefacted coatings. Possibly, these processes continued during most or all of the early Corduban Series of the West Gondwana Standard (Geyer & Landing, 2004), equivalent to the Fortunian Stage of the International Chronostratigraphic Chart (Cohen *et al.* 2013), since *Rusophycus* (Jensen *et al.* 2010) appears close to *Treptichnus pedum* (Fig. 8) almost at the base of Herrería group. Thus, the sedimentation of the Herrería group began at around 529 Ma.

e) The Cambrian succession in the Cantabrian Zone began with relatively thick conglomeratic deposits related to a forced regression resulting from the sea-level fall of the latest Ediacaran and the extensional activity as indicated by the presence in Mieldes (Fig. 1) of alluvial fans with volcanic and other rubefacted clasts filling valleys bounded by faults (Fig. 8).

f) The gradual sea-level rise began in Early Cambrian times and reached the Cantabrian Zone during the sedimentation in thickening-upward sequences of the carbonated level, or its siliciclastic equivalent, which is interpreted as the maximum flooding surface. The presence of acritarchs (Fig. 2, in Jensen *et al.* 2010) above these levels indicates the top of the Corduban or Terreneuvian Series, and hence gives an age of around 521 Ma.

Underlying and overlying these levels there are geochemical differences suggestive of a gradual increasing upward contribution of older crustal materials.

Acknowledgements

Financial support for this work was provided by the CGL2007-60035BTE and CGL2010-18905BTE projects of the MICINN (Spain). Comments by C. M. Fedo and G. Blanco improved the manuscript.

References

Ábalos, B., Puelles, P., Fernández-Armas, S. & Sarrionandia, F. 2011. EBSD microfabric study of pre-Cambrian deformations recorded in quartz pebbles from the Sierra de la Demanda (N Spain). *Journal of Structural Geology*, **33**, 500-518.

Ábalos, B., Gil-Ibarguchi, J.I., Sánchez-Lorda, M.E. & Paquette, J.L. 2012. African/ Amazonian Proterozoic correlations of Iberia: A detrital zircon U-Pb study of early Cambrian conglomerates from the Sierra de la Demanda (northern Spain). *Tectonics*, **31**, TC3003, doi: 10.1029/2011TC003041.

Álvarez Nava, H., García Casquero, J.L., Gil, A., Hernádez Urroz, J., Lorenzo, S., López Díaz, F., Mira, M., Monteserín, V., Nozal, F., Pardo, M.V., Picart, J., Robles, R., Santamaría, J. & Solé, J. 1988. Unidades litoestratigráficas de los materiales Precámbrico-Cámbrico de la mitad suroccidental de la Zona Centro Ibérica. *II Congreso Geológico de España*, **1**, Granada, 19-22.

Álvaro, J.J. & Blanc-Valleron, M.M. 2002. Stratigraphic and structural framework of the Neoproterozoic Paracuellos Group, Iberian Chains, NE Spain. *Bulletin de la Société Géologique de France*, **173**, 27-35.

Álvaro J.J., Bauluz, B., Gil Imaz, A. & Simón J.L. 2008. Multidisciplinary constraints on the Cadomian compression and early Cambrian extension in the Iberian Chains, NE Spain. *Tectonophysics*, **461**, 215-227.

Álvaro, J.J., Ezzouhairi, H., Ait Ayad, N., Charif, A., Solá, R. & Ribeiro, R. 2010. Alkaline lake systems with stromatolitic shorelines in the Ediacaran volcanosedimentary Ouarzazate Supergroup, Anti Atlas, Morocco. *Precambrian Research*, **179**, 22-36.

Aramburu, C., Truyols, J., Arbizu, M., Méndez-Bedia, I., Zamarreño, I., García-Ramos, J.C., Suárez de Centi, C. & Valenzuela, M. 1992. El Paleozoico Inferior de la Zona Cantábrica. *In*: Gutiérrez-Marco, J.C., Saavedra, J. & Rábano, I. (eds.) *Paleozoico Inferior de Ibero-América*. Universidad de Extremadura, Spain, 397-421.

Åström, M.E., Nystrand, M., Gustaffsson, J.P., Österholm, P., Nordmyr, L., Reynolds, J.K. & Peltola, P. 2010. Lanthanoid behaviour in an acidic landscape. *Geochimica et Cosmochimica Acta*, **74**, 829-845.

Avigad, D. & Gvirtzman, Z. 2009. Late Neoproterozoic rise and fall of the northern Arabian-Nubian shield: The role of lithospheric mantle delamination and subsequent thermal subsidence. *Tectonophysics*, **477**, 217-228.

Avigad, D., Sandler, A., Kolodner, K., Stern, R.J., McWilliams, M., Miller, N. & Beyth, M. 2005. Mass-production of Cambro–Ordovician quartz-rich sandstone as a consequence of chemical weathering of Pan-African terranes: environmental implications. *Earth and Planetary Science Letters,* **240**, 818–826.

Bartley, J., Pope, M., Knoll, A., Semikhatov, M. & Petrov, P. 1998. A Vendian-Cambrian boundary succession from the northwestern margin of the Siberian Platform: stratigraphy, paleontology, chemostratigraphy and correlation. *Geological Magazine*, **135**, 473-494.

Bauluz, B., Mayayo, M.J., Fernández-Nieto, C. & González López, J.M. 2000. Geochemistry of Precambrian and Paleozoic siliciclastic rocks from the Iberian Range (NE Spain): implications for source-area weathering, sorting, provenance and tectonic setting. *Chemical Geology*, **168**, 135-150.

Beratan, K.K. 1999. Miocene potassium metasomatism, Whipple Mountains, southeastern California: a database tracer of extension-related fluid transport. *Geology*, **27**, 259-262.

Bock, B., McLennan, S.M. & Hanson, G.N. 1994. Rare earth elements reditribution and its effects on the neodymium isotope system in the Austin Glen Member of the Normenskill Formation, New York, USA. *Geochimica et Cosmochimica Acta*, **58**, 5245-5253.

Bowring, S.A., Grotzinger, J.P., Condon, D.J., Ramezani, J., Newall, M.J. & Allen, P.A. 2007. Geochronologic constraints on the chronostratigraphic framework of the Neoproterozoic Huqf Supergroup, Sultanate of Oman. *American Journal of Science,* **307**, 1097-1145.

Brown, D.J., Helmke, P.A. & Clayton, M.K. 2003. Robust Geochemical Indices for Redox and Weathering on a Granitic Laterite Landscape in Central Uganda. *Geochimica et Cosmochimica Acta,* **67**, 2711-2723.

Calvet, F. & Salas, R. 1988. Tipos de plataformas carbonatadas del Precámbrico terminal de la Zona Centro Ibérica. *II Congreso Geológico de España*, **1**, Granada, 59-62.

Cohen, K.M., Finne, S.C., Gibbard, P.L. & Fan, J.X. 2013. The ICS International Chronostratigraphic chart. *Episodes*, **36**, 199-204.

Comte, P. 1959. *Recherches sur les terrains anciens de la Cordillère Cantabrique*. Memorias del Instituto Geológico y Minero de España, **60**, 440 pp.

Condie, K.C. & Wronkiewciz, D.J. 1990. The Cr/Th in Precambrian pelites from the Kaapvaal craton as an index of craton evolution. *Earth and Planetary Science Letters*, **97**, 256-267.

Cox, R., Lowe, D.R. & Cullers, R.L. 1995. The influence of sediment recycling and basement composition on evolution of mudrock chemistry in the southwestern United States. *Geochimica et Cosmochimica Acta*, **59**, 2919-2940.

Crichton J.G. & Condie, K.C. 1993. Trace elements as source indicators in cratonic sediments: A case study from the Early Proterozoic Libby Creek Group, Southeastern Wyoming. *Journal of Geology,* **101**, 319-332.

Cullers, R.L. 1994. The controls on the major and trace element variation of shales, siltstones, and sandstones of Pennsylvania-Permian age from uplifted continental blocks in Colorado to platform sediment in Kansas, USA. *Geochimica et Cosmochimica Acta*, **58**, 4955-4972.

Ennih, N. & Liégeois, J.-P. 2001. The Moroccan Anti-Atlas: the West African craton passive margin with limited Pan-African activity. Implications for the northern limit of the craton. *Precambrian Research*, **112**, 289–302.

Ennis, D.J., Dunbar, N.W., Campbell, A.R. & Chapin, C.E. 2000. The effects of K-metasomatism on the mineralogy and geochemistry of silicic ignimbrites near Socorro, New Mexico. *Chemical Geology*, **167**, 285-312.

Eriksson, K.A., Taylor, S.R. & Korsch, R.J. 1992. Geochemistry of 1.8-1.67 Ga mudstones and siltstones from the Mount Isa Inlier, Queensland, Australia: Provenance and tectonic implications. *Geochimica et Cosmochimica Acta*, **56**, 899-909.

Feng, R., Kerrich, R. & Maas, R. 1993. Geochemical, oxygen, and neodymium isotope compositions of metasediments from the Abitibi greenstone belt and Pontiac Subprovince, Canada: Evidence for ancient crust and Archean terrane yuxtaposition. *Geochimica et Cosmochimica Acta*, **57**, 641-658.

Fernández-Suárez, J., Gutiérrez-Alonso, G., Pastor-Galán, D., Hofmann, M., Murphy, J.B. & Linnemann, U. 2014. The Ediacaran-Early Cambrian detrital zircon record of NW Iberia: possible sources and paleogeographic constraints. *International Journal of Earth Sciences*, **103**, 1335-1357.

Folk, R.L. 1980. *Petrology of sedimentary rocks*. Hemphill Publishing Company, Austin, Texas.

Garrels, R.M. 1988. Sediment cycling during earth history. *In*: Lerman, M. & Meybeck, M. (eds.), *Physical and chemical weathering in geochemical cycles*. Kluwer Academic Publications, Dordrech, 341-355.

Geyer, G. & Landing, E. 2004. A unified Lower-Middle Cambrian chronostratigraphy for West Gondwana. *Acta Geologica Polonica,* **54**, 179-218.

Grew, E.S. 2002. Beryllium in Metamorphic Environments (emphasis on aluminous compositions). In: Grew, E.S. (ed.), *Beryllium: Mineralogy, Petrology and Geochemistry*. Reviews in Mineralogy and Geochemistry, **50**, 487-549.

Gutiérrez-Alonso, G., Blanco, J.A., Macfarlane, A. & Fernández-Suárez, J. 2004. Paleometeorización vs. paleoalteración en la superficie de discordancia Proterozoico-

Cámbrico en el antiforme de Narcea. *Geogaceta,* **36**, 320-336.

Harlavan, Y., Erel, Y. & Blum, J.D. 2009. The coupled release of REE and Pb to the soil labile pool with time by weathering of accessory phases, Wind River Mountains, WY. *Geochimica et Cosmochimica Acta,* **73**, 320-336.

Hu, Z. & Gao, S. 2008. Upper crustal abundances of trace elements: a revision and update. *Chemical Geology,* **253**, 205–221.

Hutcheon, I., Bloch, J., Caritat, P., de Shevalier, M., Abercrombie, H. & Longstaffe, F. 1998. What is the cause of potassium enrichment in shales? *In*: Schieber, J., Zimmerle, W.S. & Sethi, P.S. (eds.), *Shales and mudstones II.* E. Schweizerbart'sche Verlagsbuchhandlung, Stuttgart, 107-128.

Jahn, B. M. & Condie, K.C. 1995. Evolution of the Kaapvaal Craton as viewed from geochemical and Sm-Nd isotopic analyses of intracontinental pelites. *Geochimica et Cosmochimica Acta,* **59**, 2239-2258.

Jensen, S., Palacios, T. & Martí Mus, M. 2010. Revised biochronology of the Lower Cambrian of the Central Iberian zone, southern Iberian massif, Spain. *Geological Magazine*, **147**, 690-703.

Johnson, P.R., Andresen, A., Collins, A.S., Fowler, A.R., Fritz, H., Ghebreab, W., Kusky, T. & Stern, R.J. 2011. Late Cryogenian-Ediacaran history of the Arabian-Nubian Shield: A review of depositional, plutonic, structural, and tectonic events in the closing stages of the northern East African Orogen. *Journal of African Earth Sciences,* **61**, 167-232.

Knoll, A.H., Walter, M.R., Narbonne, G.M. & Christie-Blick, N. 2004. A new period for the geologic time scale. *Science*, **305**, 621-622.

Leising, J.F., Tyler, S.W. & Miller, W.W. 1995. Convection of saline brines in enclosed lacustrine basins: a mechanism for potassium metasomatism. *Geological Society of America Bulletin,* **107**, 1157-1163.

Liñán, E. & Tejero, R. 1988. Las formaciones precámbricas del antiforme de Paracuellos (Cadenas Ibéricas). *Boletín de la Real Sociedad de Historia Natural*, **84**, 39-

49.

Liñán, E., Gozalo, R., Palacios, T., Gámed-Vintaned, J.A., Ugidos, J.M. & Mayoral, E. 2002. Cambrian. *In*: Gibbons, W. & Moreno, T. (eds.), *The Geology of Spain*. Geological Society, London, 17-29.

Martín Parra, L.M., Enrile A., González Lastra, J., Maymo, A. & Bardají, M.T. 1989. *Memoria y Mapa geológico de la Hoja nº 128 (Riello) del Mapa geológico de España a escala 1:50000 (2ª serie)*. Instituto Geológico y Minero de España, Madrid, Spain.

McLennan, S.M. 1989. Rare earth elements in sedimentary rocks: influence of provenance and sedimentary processes. *Reviews in Mineralogy,* **21**, 169-200.

McLennan, S.M., Taylor, S.R., McCulloch, M.T. & Maynard, J.B. 1990. Geochemical and Nd-Sr isotopic composition of deep-sea turbidites: Crustal evolution and plate tectonic associations. *Geochimica et Cosmochimica Acta*, **54**, 2015-2050.

McLennan, S.M., Hemming, S., McDaniel, D.K. & Hanson, G.N. 1993. Geochemical approaches to sedimentation, provenance, and tectonics. *In*: Johnsson, M.J. & Basu, A. (eds.), *Processes Controlling the Composition of Clastic Sediments*. Geological Society of America. Colorado, Special Paper, **284**, 21-40.

McLennan, S.M., Hemming, S.R., Taylor, S.R. & Eriksson, K.A. 1995. Early Proterozoic crustal evolution: Geochemical and Nd-Pb isotopic evidence from metasedimentary rocks, southwestern North America. *Geochimica et Cosmochimica Acta,* **59**, 1153-1177.

McLennan, S.M., Taylor, S.R. & Hemming, S.R. 2006. Composition, differentiation, and evolution of continental crust: constraints from sedimentary rocks and heat flow. *In*: Brown, M. & Rushmer, T. (eds.), *Evolution and Differentiation of the Continental Crust*. Cambridge University Press, 92-134.

Munz, I.A., Yardley, B.W.D., Banks, D.A. & Wayne, D. 1995. Deep penetration of sedimentary fluids in basement rocks from southern Norway: Evidence from hydrocarbon and brine inclusions in quartz veins. *Geochimica et Cosmochimica Acta*, **59**, 239-254.

Nesbitt, H.W. & Young, G.M. 1982. Early Proterozoic climates and plate motions inferred from major elements chemistry of lutites. *Nature*, **299**, 715-717.

Páez, G.N., Ruiz, R., Guido, D.M., Jovic, S.M. & Schalamuck, I.B. 2010. The effects of K-metasomatism in the Bahía Laura Volcanic Complex, Deseado Massif, Argentina: petrologic and metallogenetic consequences. *Chemical Geology*, **273**, 300-313.

Palacios, T. & Vidal, G. 1992. Lower Cambrian acritarchs from Northern Spain: the Precambrian-Cambrian boundary and biostratigraphic implications. *Geological Magazine*, **129**, 421-436.

Parga, J.R. & Luque, C. 1971. Las series del Cámbrico Inferior y Eocámbrico en la Cordillera Cantábrica. *Boletín Geológico y Minero*, **83**, 310-320.

Parnell, J., Mark, D.F., Frei, R., Fallick, A.E. & Ellam, R.M. 2014. ^{40}Ar/^{39}Ar dating of exceptional concentration of metals by weathering of Precambrian rocks at the Precambrian-Cambrian boundary. *Precambrian Research*, **246**, 54-63

Pérez Estaún, A. 1978. Estratigrafía y estructura de la rama Sur de la Zona Asturoccidental-Leonesa. *Memorias del Instituto Geológico y Minero de España*, **92**, 1-149.

Pérez Estaún, A., Bastida, F., Martínez Catalán, J.R., Gutiérrez Marco, J.C., Marcos, A. & Pulgar, J.A. 1990. West Asturian-Leonese Zone: Stratigraphy. *In*: Dallmeyer, R.D. & Martínez-García, E. (eds.), *Pre-Mesozoic Geology of Iberia*. Springer, Berlin, 92-102.

Piqué, A. 2003. Evidence for an important extensional event during the Latest Proterozoic and Earliest Paleozoic in Morocco. *Comptes Rendus Geoscience,* **335**, 865-868.

Pyle, L.J., Narbonne, G.M., James, N.P., Dalrymple, R.W. & Kaufman, A.J. 2004. Integrated Ediacaran chronostratigraphy, Wernecke Mountains, northwestern Canada. *Precambrian Research*, **132**, 1-27.

Rubio-Ordóñez, A. 2010. *Magmatismo Neoproterozoico en el Antiforme del Narcea*. Ph.D. thesis, Universidad de Oviedo, Spain, 306 pp.

Rubio-Ordóñez, A., Barba, P., Cuesta, A., Gallastegui, G., Suárez, O., Ugidos, J.M. & Valladares, M.I. 2004. Los cantos volcánicos del conglomerado basal de la Fm. Herrería: Evidencias de un volcanismo Neoproterozoico en la base del Cámbrico. *Geogaceta*, **36**, 11-14.

Rubio-Ordóñez, A., Gallastegui, G., Suárez, O., Pupin, J-P. & Corretgé, L.G. 2006. Zircon morphology vs. whole-rock geochemical characterization in meta-volcanic rocks. *Geophysical Research Abstracts*, **8**, 08947.

Rubio-Ordoñez, A., Gutiérrez Alonso, G., Valverde-Vaquero, P., Cuesta, A., Gallastegui, G., Gerdes, A. & Cárdenes, V. 2015. Arc-related Ediacaran magmatism along the northern margin of Gondwana. Geochronology and isotopic geochemistry from northern Iberia. *Gondwana Research*, **27**, 216-227.

Rudnick, R.L. & Gao, S., 2005. Composition of the continental crust. *In*: Rudnick, R.L. (ed.), *The Crust*, Treatise on Geochemistry, Vol. 3, 1-64.

Ryan, J.G. 2002. Trace-Element systematics of Beryllium in Terrestrial Materials. *In*: Grew E.S. (ed.), *Beryllium: Mineralogy, Petrology and Geochemistry*. Reviews in Mineralogy and Geochemistry, **50**, 121-145.

Sandler, A. & Harlavan, Y. 2006. Early diagenetic illitization of illite-smectite in Cretaceous sediments (Israel): evidence from K-Ar dating. *Clay Minerals*, **41**, 637-658.

Sandler, A., Teutsch, N. & Avigad, D. 2012. Sub-Cambrian pedogenesis recorded in weathering profiles of the Arabian-Nubian Shield. *Sedimentology*, **59**, 1305-1320.

Saylor, B.Z. 2003. Sequence stratigraphy and carbonate-siliciclastic mixing in a terminal Proterozoic foreland basin, Urusis Formation, Nama Group, Namibia. *Journal of Sedimentary Research*, **73**, 264-279.

Schock, H.H. 1975. Geochemistry and Mineralogy. *In*: Horovitz, C. T. (ed.), *Scandium*. Its occurrence, Chemistry, Physics, Metallurgy, Biology and Technology. Academic Press, London, 50-65.

Scribner, A.M., Kurtz, A.C. & Chadwick, O.A. 2006. Germanium sequestration by soil: Targeting the roles of secondary clays and Fe-oxyhydroxides. *Earth Planetary Science*

Letters, **243**, 760-770.

Shields, G.A. 2007. A normalised seawater strontium isotope curve: possible implications for Neoproterozoic-Cambrian weathering rates and further oxygenation of the Earth. *eEarth,* **2**, 35-42.

Soulaimani, A., Essaifi, A., Youbi, N. & Hafid, A. 2004. Les marqueurs structuraux et magmatiques de l'extension crustale au Protérozoïque terminal–Cambrien basal autour du massif de Kerdous (Anti-Atlas occidental, Maroc). *Comptes Rendus Geoscience*, **336**, 1433-1441.

Tassinari, C.C.G., Medina, J. & Pinto, M.S. 1996. Rb-Sr and Sm-Nd geochronology and isotope geochemistry of Central Iberian metasedimentary rocks (Portugal). *Geologie en Mijnbouw,* **75**, 69-79.

Thomas, R.J., Fekkak, A., Ennih, N., Errami, E., Loughlinc, S.C., Gresse, P.G., Chevallier, L.P. & Liégéois, J.-P. 2004. A new lithostratigraphic framework for the Anti-Atlas Orogen, Morocco. *Journal of African Earth Sciences*, **39**, 217-226.

Torres, J., Droz, L., Savoye, B., Terentieva, E., Cochonat, P., Kenyon, N.H. & Canals, M. 1997. Deep-sea avulsion and morphosedimentary evolution of the Rhône Fan Valley and Neofan during the Late Quaternary (north-western Mediterranean Sea). *Sedimentology,* **44**, 457-477.

Ugidos, J.M., Valladares, M.I., Recio, C., Rogers, G., Fallick, A.E. & Stephens, W.E. 1997a. Provenance of Upper Precambrian-Lower Cambrian shales in the Central Iberian Zone, Spain: evidence from a chemical and isotopic study. *Chemical Geology*, **136**, 55-70.

Ugidos, J.M., Armenteros, I., Barba, P., Valladares, M.I. & Colmenero, J.R. 1997b. Geochemistry and petrology of recycled orogen-derived sediments: a case study from Upper Precambrian siliciclastic rocks of the Central Iberian Zone, Iberian Massif, Spain. *Precambrian Research,* **84**, 163-180.

Ugidos, J.M., Stephens, W.E., Carnicero, A. & Ellam, R.M. 2008. A reactive assimilation model for regional-scale cordierite-bearing granitoids: geochemical evidence from the Late Variscan granites of the Central Iberian Zone, Spain. *Earth and*

Environmental Science Transactions of the Royal Society of Edinburgh, **99**, 225-250.

Ugidos, J.M., Sánchez-Santos, J.M., Barba, P. & Valladares, M.I. 2010. Upper Neoproterozoic series in the Central Iberian, Cantabrian and West Asturian Leonese Zones (Spain): geochemical data and statistical results as evidence for a shared homogenised source area. *Precambrian Research*, **178**, 51-58.

Valladares, M.I. 1995. Siliciclastic-carbonate slope apron in an immature tensional margin (Upper Precambrian-Lower Cambrian), Central Iberian Zone, Salamanca, Spain. *Sedimentary Geology,* **94**, 165-186.

Valladares, M.I., Barba, P., Ugidos, J.M. Colmenero, J.R. & Armenteros, I. 2000. Upper Neoproterozoic-Lower Cambrian sedimentary successions in the Central Iberian Zone (Spain): sequence stratigraphy, petrology and chemostratigraphy. Implications for other European zones. *International Journal of Earth Sciences*, **89**, 2-20.

Valladares, M.I., Barba, P. & Ugidos, J.M. 2002a. Precambrian. *In*: Gibbons, W. & Moreno, T. (eds.), *The Geology of Spain*. Geological Society, London, 7-16.

Valladares, M.I., Ugidos, J.M., Barba, P. & Colmenero J.R. 2002b. Contrasting geochemical features of the Central Iberian Zone shales (Iberian Massif, Spain): Implications for the evolution of Neoproterozoic-Lower Cambrian sediments and their sources in other Peri-Gondwanan areas. *Tectonophysics,* **352**, 121-132.

Valladares, M.I., Ugidos, J.M., Barba, P., Fallick, A.E. & Ellam, R.M. 2006. Oxygen, carbon and strontium isotope records of Ediacaran carbonates in Central Iberia (Spain). *Precambrian Research,* **147**, 354-365.

van der Bosch, W.J. 1969. Geology of the Luna-Sil region, Cantabrian Mountains (Spain). *Leidse Geologische Mededelingen*, **44**, 137-225.

Vidal, G., Palacios, T., Gámed-Vintaned, J.A., Díez Balda, M.A. & Grant, S.W. 1994. Neoproterozoic-early Cambrian geology and paleontology of Iberia. *Geological Magazine*, **131**, 729-765.

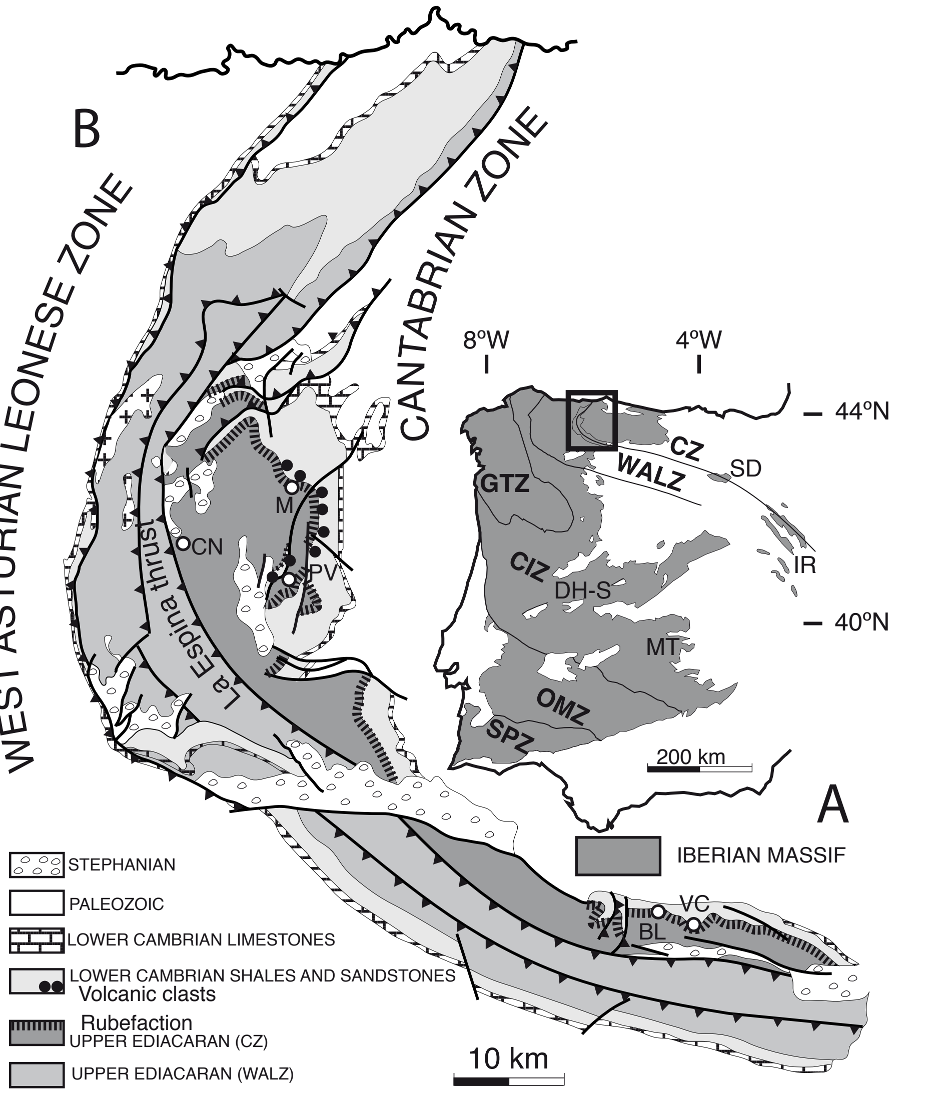

Fig. 1. (A) Zoning of the Iberian Massif, CZ: Cantabrian Zone; WALZ: West Asturian-Leonese Zone; GTZ: Galicia Tras os Montes Zone; CIZ: Central Iberian Zone; OMZ: Ossa Morena Zone; SPZ: South Portuguese Zone; IR: Iberian Range; SD: Sierra de la Demanda; DH-S: Domo de las Hurdes-Salamanca; MT: Montes de Toledo. (B) Geological map of the Narcea antiform in the Iberian Massif. BL: Barrios de Luna, CN: Cangas del Narcea, M: Mieldes, PV: Parada la Vieja, VC: Vega de los Caballeros.

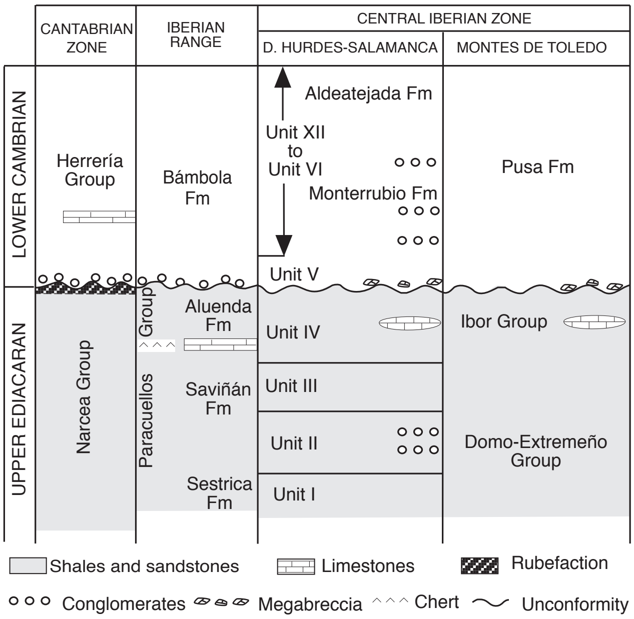

Fig. 2. Simplified correlation chart of the lithostratigraphic units of the Late Ediacaran-Early Cambrian of the Cantabrian, Central Iberian zones and Iberian Ranges (Valladares et al. 2002a and references therein).

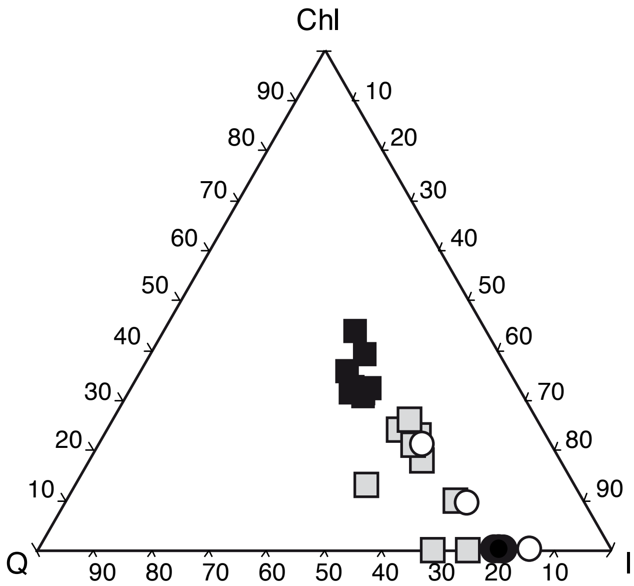

Fig. 3. Plot of the main mineral components of the shales studied. The diagram separates the Upper Ediacaran shales (filled squares) from the rubefacted equivalents (grey squares) and Lower Cambrian (filled and open circles: underlying and overlying shales, respectively. See text). Chl: chlorite; I: illite; Q: quartz.

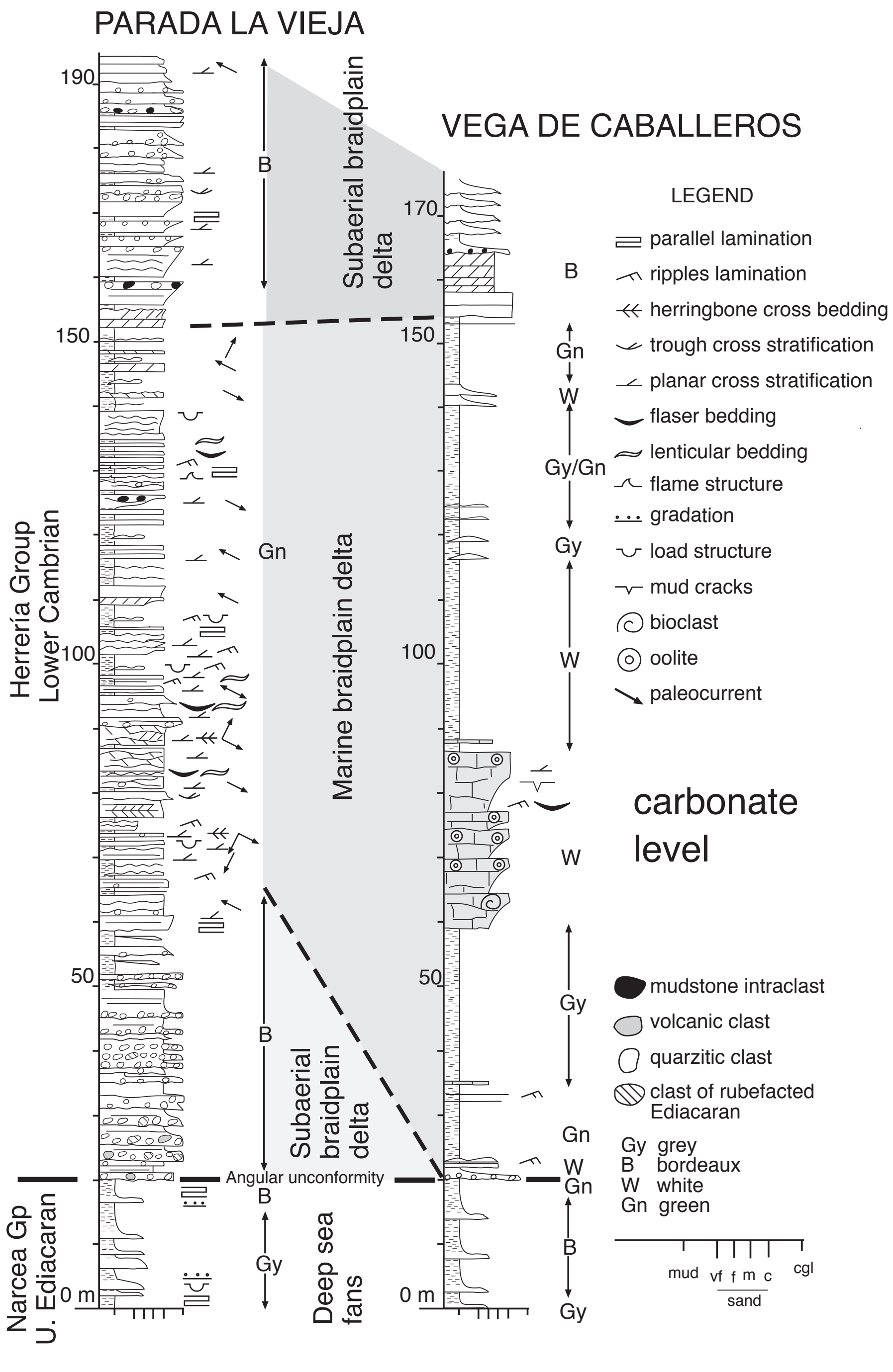

Fig. 4. Stratigraphic logs of the basal Herería group in the two sections studied: Parada la Vieja (PV, Fig. 1B) and Vega de Caballeros (VC, Fig. 1B) showing that the carbonated level present in VC is absent in PV. Both sections have three intervals showing braidplain delta features.

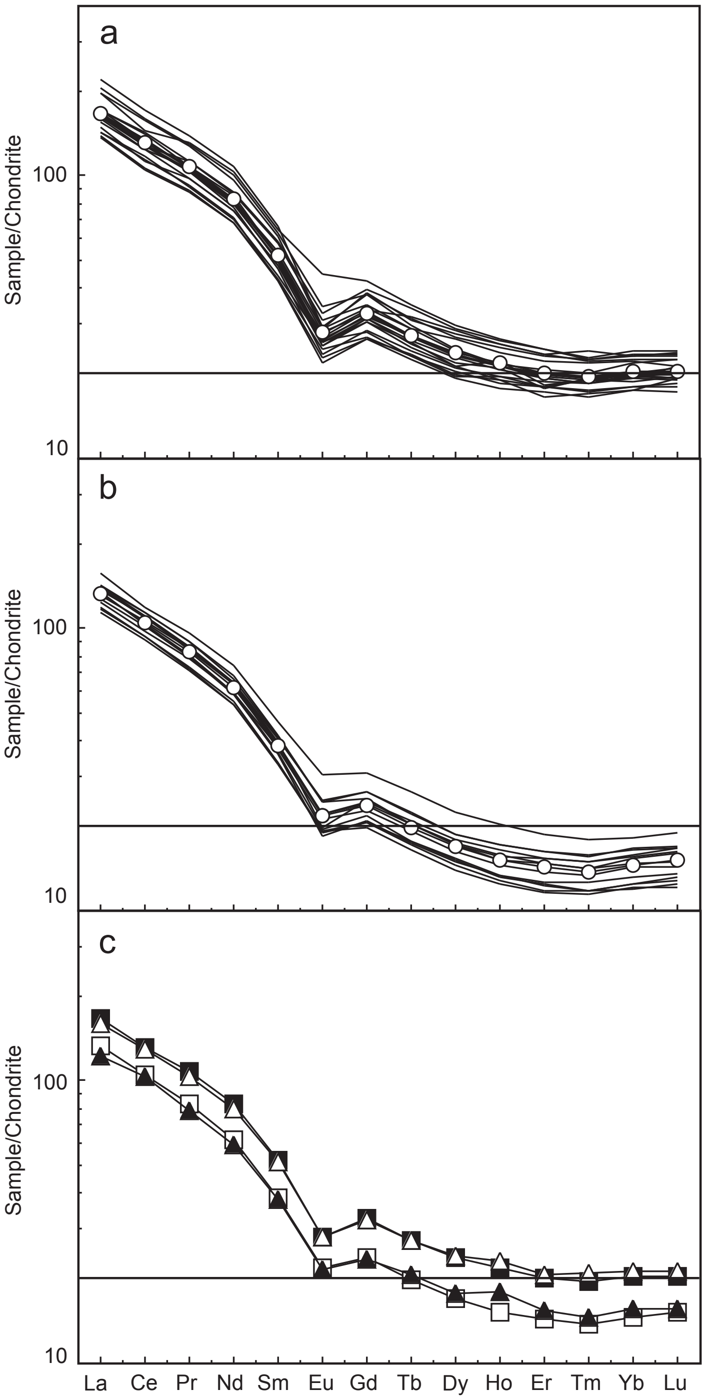

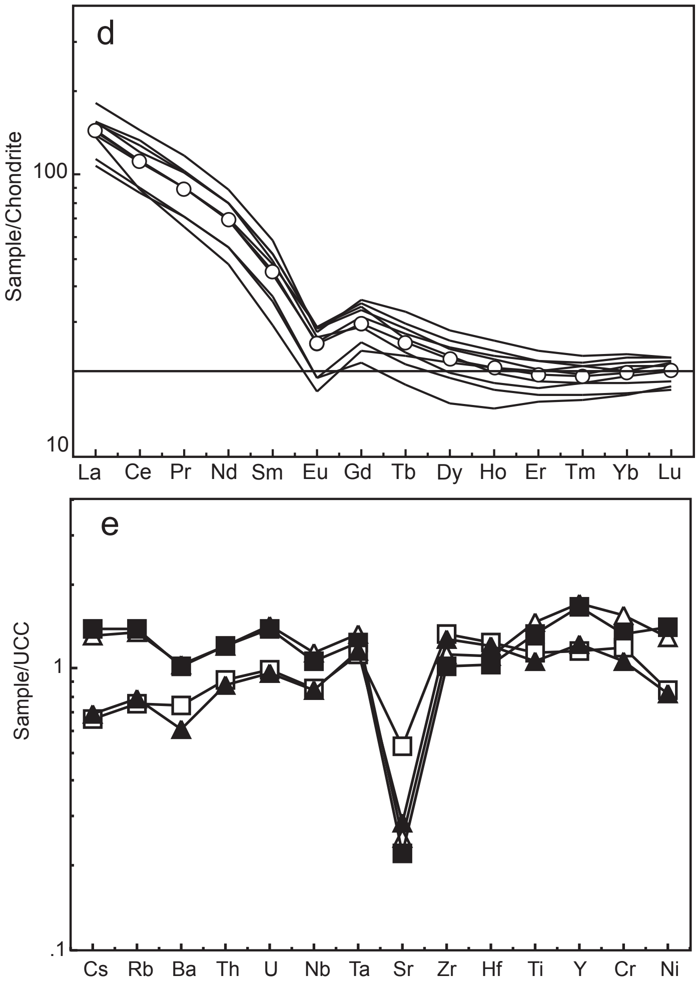

Fig. 5. Chondrite normalised REE patterns for the Ediacaran shales (a), sandstones (b), NIBAS and the mean (n=16) sandstone (c) of the Central Iberian Zone. Upper Continental Crust (UCC) normalised multi-element diagram (d). Chondrite normalised REE patterns for the rubefacted shales (e). Circles: mean patterns. Filled and open squares: mean Ediacaran shales and sandstones, respectively. Open and filled triangles: NIBAS and the mean sandstone, respectively.

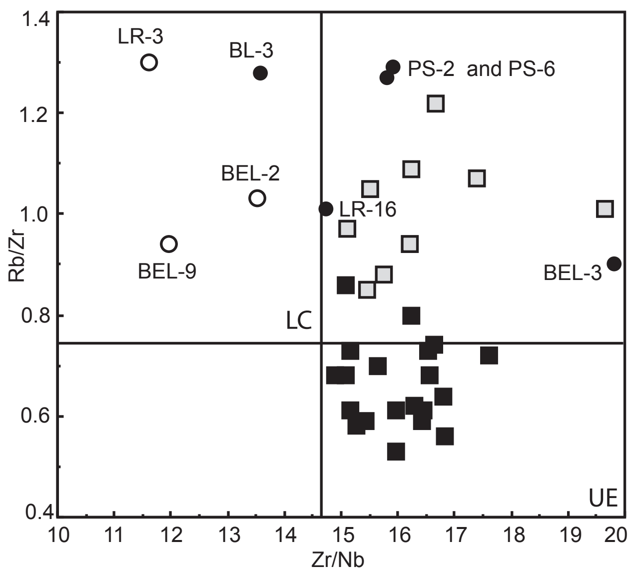

Fig. 6. Diagram Zr/Nb-Rb/Zr. The all the Ediacaran shales (filled squares), including the rubefacted equivalents (grey squares), show relatively high Zr/Nb ratios characteristic of the Ediacaran shales in the Central Iberian Zone (field UE). However, only the Lower Cambrian shales overlying the carbonate level (samples LR-3, BEL-2, BEL-9) plot in the Cambrian field (LC) while all the samples underlying this level (filled circles) but one show Zr/Nb ratios typical of the Ediacaran field but Rb/Zr ratios as high as those of the rubefacted shales. See text. UE and LC: fields of the Upper Ediacaran and Lower Cambrian shales in the Central Iberian Zone (Valladares et al. 2002b). Symbols as in Fig. 3.

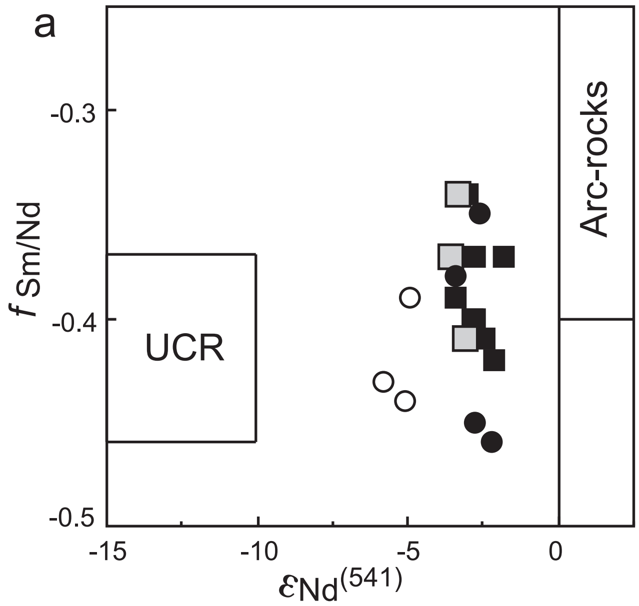

Fig. 7a. εNd(t)-fSm/Nd diagram (after Bock et al. 1994, simplified). Plots of Ediacaran and underlying Lower Cambrian shales are consistent with the inheritance of homogenised mixtures of upper-crustal and juvenile compositions and the increase of the proportion of the upper crustal rocks in the overlying Lower Cambrian shales. UCR: Upper-crustal rocks. Symbols as in Fig. 3.

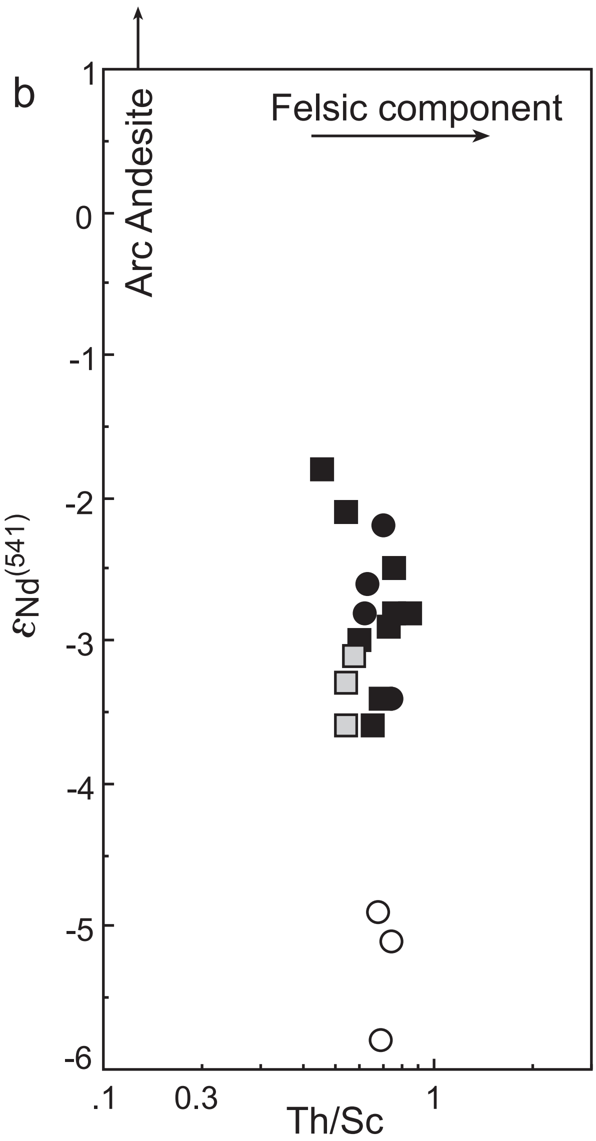

Fig. 7b. Th/Sc-εNd(t) diagram (McLennan et al. 1993) consistently favouring the interpretation that Ediacaran detrital rocks would consist of inherited homogenised mixtures of juvenile and crustal components and a higher proportion of the latter ones in the Lower Cambrian sediments. Symbols as in Fig. 3.

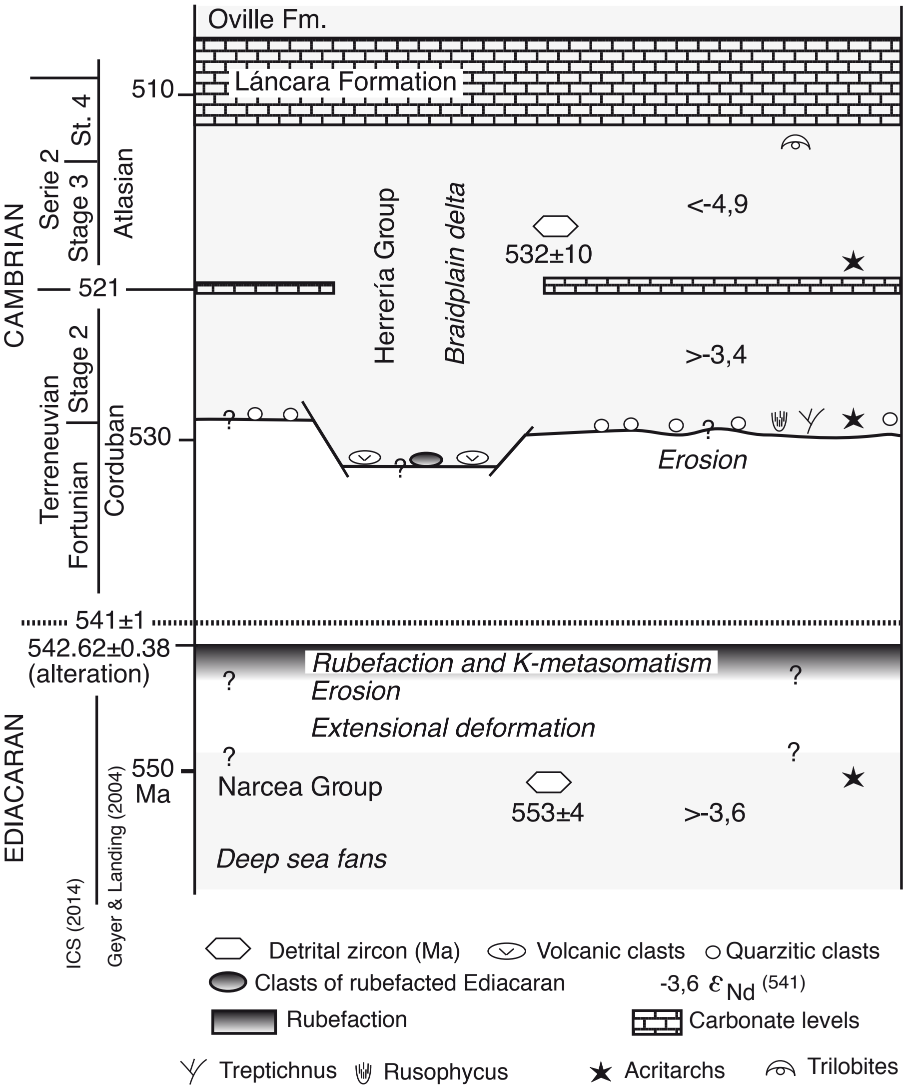

Fig. 8. Chronostratigraphic framework of the Ediacaran-Lower Cambrian boundary in the Cantabrian Zone and sedimentary, geochemical and tectonic processes produced. Note that the vertical scale indicates time, not thickness.

Table 1. *Mineral (%) semi-quantitative analyses (XRD) of the shales studied*

Sample	Group	Quartz	Albite	Chlorite	Illite	K-feldspar	Other
BEL-2	OLC	12	0	0	76	12	-
BEL-9	0LC	19	0	9	68	4	-
LR-3	OLC	22	0	22	57	-	-
BL-3	ULC	20	0	0	80	-	-
PS-2	ULC	18	0	0	82	-	-
PS-6	ULC	19	0	0	81	-	Hematite
BEL-23	RUE	21	0	23	56	-	Hematite
BEL-7	RUE	24	0	0	76	-	Hematite
BL-5	RUE	35	0	13	52	-	Hematite
BL-6	RUE	21	0	26	52	-	Hematite
LR-14	RUE	23	0	21	56	-	Hematite
LR-15	RUE	21	0	10	69	-	Hematite
PS-16	RUE	30	0	0	70	-	Hematite
PS-3	RUE	24	0	24	51	-	-
PS-4	RUE	23	0	18	59	-	-
BEL-1	UE	17	12	30	41	-	Hematite
BEL-5	UE	19	14	37	29	-	-
BEL-6	UE	20	13	34	33	-	-
BL-1	UE	24	13	31	32	-	-
BL-13	UE	22	13	28	36	-	-
BL-14	UE	25	14	27	34	-	-
LR-5	UE	24	13	27	37	-	-
LR-7	UE	24	14	28	34	-	-
LR-8	UE	23	15	27	36	-	-

UCL and OCL Lower Cambrian, samples underlying and overlying, the carbonate level, respectively.
RUE: Rubefacted Upper Ediacaran.
UE: Upper Ediacaran.

Table 2. *Model compositional changes (%) of element concentrations of the rubefacted Ediacaran shales from the Cantabrian Zone, N Spain. Change 1 and 2: % differences between RUE and UE median and mean values, respectively. Negative values indicate depletion.*

	Median UE	Median RUE	Change 1	Mean UE	Mean RUE	Change 2
SiO_2	60.45	60.46	0.02	59.84	61.02	1.98
TiO_2	0.86	0.88	2.33	0.85	0.84	-1.39
Al_2O_3	18.14	18.81	3.69	18.32	18.36	0.20
Fe_2O_3	7.05	7.08	0.43	7.10	6.96	-1.99
MgO	2.96	2.09	-29.4	3.02	2.03	-32.8
CaO	0.43	0.11	-74.4	0.48	0.16*	-71.1
Na_2O	2.22	0.07*	-96.9	2.22	0.10*	-95.5
K_2O	3.60	5.73	59.2	3.77	5.63	49.5
P_2O_5	0.24	0.22	-8.33	0.24	0.20	-17.7
Rb	128	190	48.4	130	197	51.5
Cs	6.62	21.6	226	6.82	18.2	166
Be	3.00	2.62	-12.67	3.16	2.83	-10.3
Sr	67.0	15.7	-76.6	70.3	15.5	-77.9
La	40.7	35.7	-12.3	41.2	35.3	-14.3
Ce	81.6	71.3	-12.6	83.1	71.2	-14.3
Pr	10.2	8.70	-14.7	10.3	8.69	-16.0
Nd	39.1	34.0	-13.0	40.2	33.7	-16.1
Sm	7.95	7.49	-5.79	8.16	7.07	-13.4
Eu	1.58	1.58	0.00	1.67	1.47	-9.71
Gd	6.67	6.50	-2.55	6.86	6.22	-9.34
Tb	1.02	0.99	-2.94	1.04	0.96	-7.33
Dy	5.96	5.86	-1.68	6.09	5.74	-5.88
Ho	1.16	1.13	-2.59	1.20	1.13	-5.90
Er	3.24	3.36	3.70	3.35	3.26	-2.54
Tm	0.49	0.51	4.08	0.51	0.50	-1.94
Yb	3.33	3.41	2.40	3.44	3.35	-2.53
Lu	0.52	0.54	3.85	0.53	0.53	-0.93
Y	34.0	32.6	-4.12	34.8	33.1	-4.84
Sc	18.3	20.3	10.9	19.0	19.5	3.02
Th	12.8	11.1	-13.3	12.6	11.2	-10.9
U	3.60	3.21	-10.8	3.61	3.12	-13.5
Nb	12.7	13.0	2.36	12.4	12.0	-3.27
Co	19.0	14.6	-21.1	19.0	16.0	-14.4
Ni	49.0	41.0	-16.3	48.0	41.0	-14.4
Cu	41.0	4.22	-89.7	39.0	7.83*	-20.7
Zn	104	74.9	-27.9	107	71.0	-33.5
Ge	1.75	2.13	21.9	1.74	2.09	19.7
Pb	10.9	5.76	-47.2	14.9	5.30	-64.5
As	18.5	2.13	-88.5	20.0	3.03*	-84.8

UE: Ediacaran shales. RUE: Rubefacted UE. *Calculated accepting detection limits as maximum abundances of the elements

Table 3. *Synthesis of the mean element ratio values and standard deviations of the shales and sandstones from the Cantabrian and Central Iberian zones*

Rock groups	1	2	3	4	5	6	7	8
Samples	(n=20)	(n=100)	(n=13)	(n=16)	UCC	(n=9)	(n=5)	(n=3)
Al_2O_3/TiO_2	21.80(2.2)	20.48(1.43)	19.39(2.14)	18.85(1.03)	24.06	22.57(4.01)	24.46(2.87)	24.25(2.02)
K_2O/Al_2O_3	0.223 (0.01)	0.215(0.02)	0.169(0.03)	0.166(0.02)	0.197	0.333(0.02)	0.370(0.01)	0.431(0.08)
Rb/Sr	1.93(0.37)	1.72(0.58)	0.45(0.13)	0.51(0.11)	0.29	13.75(3.85)	10.90(8.97)	3.21(0.64)
Cs/Be	2.18(0.48)	2.38(0.73)	1.67(0.33)	1.86(0.48)	2.58	6.69(3.37)	6.66(1.73)	3.03(1.38)
Ti/Zr	25.76(1.62)	26.08(1.86)	17.23(2.61)	16.90(3.12)	19.88	25.63(3.89)	24.34(2.82)	30.77(1.22)
Ti/Nb	411(21.80)	429(29.89)	440(25.22)	422(34.22)	331	418(47.38)	384(20.6)	379(19.0)
La/Sc	2.19(0.33)	1.93(0.31)	2.83(0.28)	nd	2.21	1.83(0.32)	2.13(0.16)	2.41(0.21)
Th/Sc	0.67(0.09)	0.62(0.10)	0.83(0.11)	nd	0.75	0.58(0.06)	0.68(0.05)	0.70(0.04)
La/Cr	0.43(0.03)	0.35/0.06)	0.38(0.03)	0.39(0.05)	0.42	0.38(0.07)	0.48(0.04)	0.50(0.04)
Cr/Th	7.69(0.76)	9.07(1.41)	9.09(0.81)	8.55(0.82)	6.95	8.39(1.28)	6.65(0.66)	6.92(0.37)
Zr/Hf	35.90(1.12)	36.96(1.46)	39.28(0.87)	38.56(2.49)	36.42	36.23(0.74)	35.80(0.86)	36.35(0.58)
Zr/Sc	10.48(1.08)	10.65(1.49)	22.36(4.63)	nd	10.9	10.11(1.29)	10.19(1.76)	7.82(0.68)
Zr/Nb	15.96(0.75)	16.49(1.23)	26.02(3.59)	25.54(3.65)	16,6	16.45(1.40)	15.96(2.36)	12.36(1.02)
Th/Nb	1.03(0.09)	0.96(0.10)	0.97(0.07)	0.94(0.09)	0.90	0.95(0.07)	1.06(0.08)	1.11(0.01)
$(La/Yb)_N$	8.21(0.69)	7.44(0.99)	9.14(0.78)	7.84(1.05)	8.95	7.23(0.77)	7.33(0.83)	9.26(1.03)
Eu/Eu*	0.67(0.6)	0.70(0.05)	0.72(0.04)	0.73(0.03)	0.70	0.67(0.04)	0.62(0.04)	0.69(0.03)
Rb/Th	10.33(1.16)	10.01(1.18)	7.37(1.08)	8.04(1.36)	8.95	17.56(2.08)	17.01(1.34)	12.13(1.85)
Rb/Zr	0.66(0.08)	0.58(0.08)	0.28(0.05)	0.30(0.07)	0.49	1.01(0.11)	1.15(0.18)	1.09(0.19)

1: Ediacaran shales. 2: NIBAS (Ugidos *et al.* 2010), Sc: 72 analyses. 3: Ediacaran sandstones. 4 Ediacaran sandstones from the Central Iberian Zone (Ugidos *et al.* 1997b), nd: no data of Sc. 5: Upper Continental Crust (UCC, Rudnick & Gao 2005; Hu & Gao 2008). 6: Rubefacted shales. 7 and 8: Lower Cambrian shales underlying and overlying, respectively, the carbonate level (see text). N: chondrite (Pourmand *et al.* 2012) normalised.

Table 4. *Sm and Nd contents (ppm) and Nd isotope data of the Ediacaran and Lower Cambrian shales.*

Samples No.	Sm	Nd	$^{147}Sm/^{144}Nd$	$^{143}Nd/^{144}Nd$	2se	εNd (t)	$f_{Sm/Nd}$	TDM (Ga)
OLC								
BEL-2*	8.52	45.8	0.1125	0.512041	6	-5.8	-0.43	1.61
LR-3*	8.07	40.8	0.1196	0.512268	5	-4.9	-0.39	1.62
BEL-9	7.97	43.4	0.1111	0.512069	11	-5.1	-0.44	1.55
ULC								
BL-3*	9.10	42.3	0.1301	0.512268	6	-2.6	-0.34	1.54
BEL-3*	6.44	34.2	0.1140	0.512236	6	-2.1	-0.42	1.35
LR-16*	8.43	41.5	0.1229	0.512199	5	-3.4	-0.38	1.54
PS-2*	8.23	45.7	0.1087	0.511798	6	-2.8	-0.45	1.36
RUE								
LR-14*	7,53	35,1	0.1298	0.512232	7	-3.3	-0.34	1.60
BEL-7*	4,52	23,5	0.1161	0.512196	5	-3.1	-0.41	1.44
PS-4*	5,82	28,5	0.1234	0.512192	6	-3.6	-0.37	1.56
UE								
BEL-1	9.53	46.8	0.1232	0.512195	6	-3.6	-0.37	1.55
BEL-5*	8.61	42.3	0.1231	0.512284	5	-1.8	-0.37	1.40
BEL-11*	9.91	52.5	0.1142	0.512238	7	-2.1	-0.42	1.35
CN-1	8.97	41.9	0.1295	0.512244	7	-3.0	-0.34	1.58
BL-11	7.68	38.8	0.1197	0.512191	3	-3.4	-0.39	1.50
LR-1	7.70	39.3	0.1185	0.512214	7	-2.9	-0.40	1.45
VIL-1	6.93	33.9	0.1237	0.512235	8	-2.8	-0.37	1.49
BL-1	8.06	41.5	0.1176	0.512215	7	-2.8	-0.40	1.43
BL-2	6.67	34.6	0.1166	0.512228	7	-2.5	-0.41	1.40

Nd isotope analyses at SGIker-Geochronology and Isotopic Geochemistry (*), University of the Basque Country (Spain) and at SUERC, East Kilbride (UK). OCL and UCL: Lower Cambrian, samples overlying and underlying, respectively, the carbonate level. See text. RUE: Rubefacted Upper Ediacaran. UE: Upper Ediacaran.

Suplementary Fig. 1. Representative diffractograms ºof the shales studied showing the main mineralogical results.
Chl: chlorite; I: illite; Ph: phyllosilicates; Q: quartz; Alb: albite; H: Hematite;
KF: K-feldspar; Ph060: 060 reflection of phyllosilicates.
Top right corner: Detail of the XRD patterns of the <2µm fraction of a representative sample (LR-8) containing chlorite (14Å and 7Å) and illite (10 Å). OA: oriented aggregates; EG: treated with ethylene-glycol; C: calcinated.

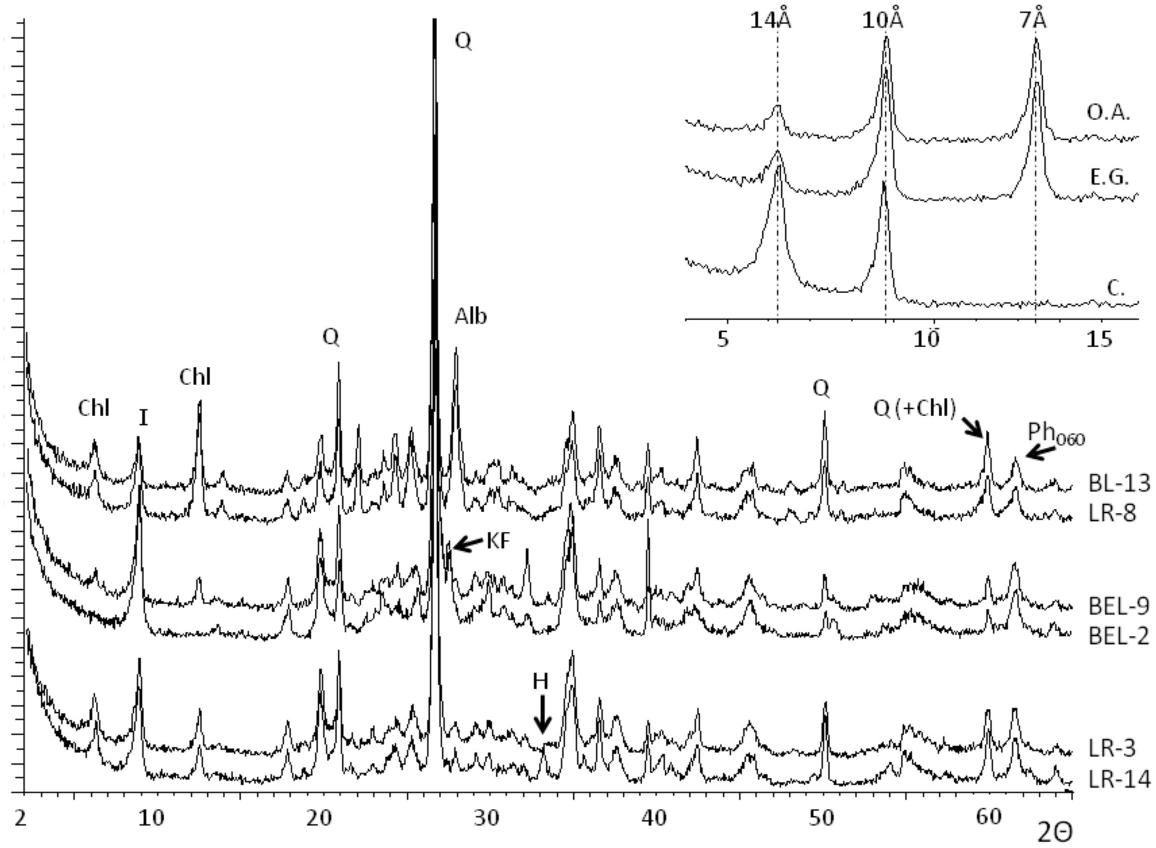

Supplementary Fig. 2. Chondrite-normalised REE patterns for the Ediacaran shales (a) and sandstones (b). Open circles: mean patterns. (c) REE patterns of the mean Ediacaran shales (filled squares) and sandstones (open squares) from the Cantabrian Zone, NIBAS (open triangle) and the mean (n=16) sandstone (filled triangles) of the Central Iberian Zone. Normalising chondrite values after Pourmand *et al.* 2012. Symbols as in Fig. 3.

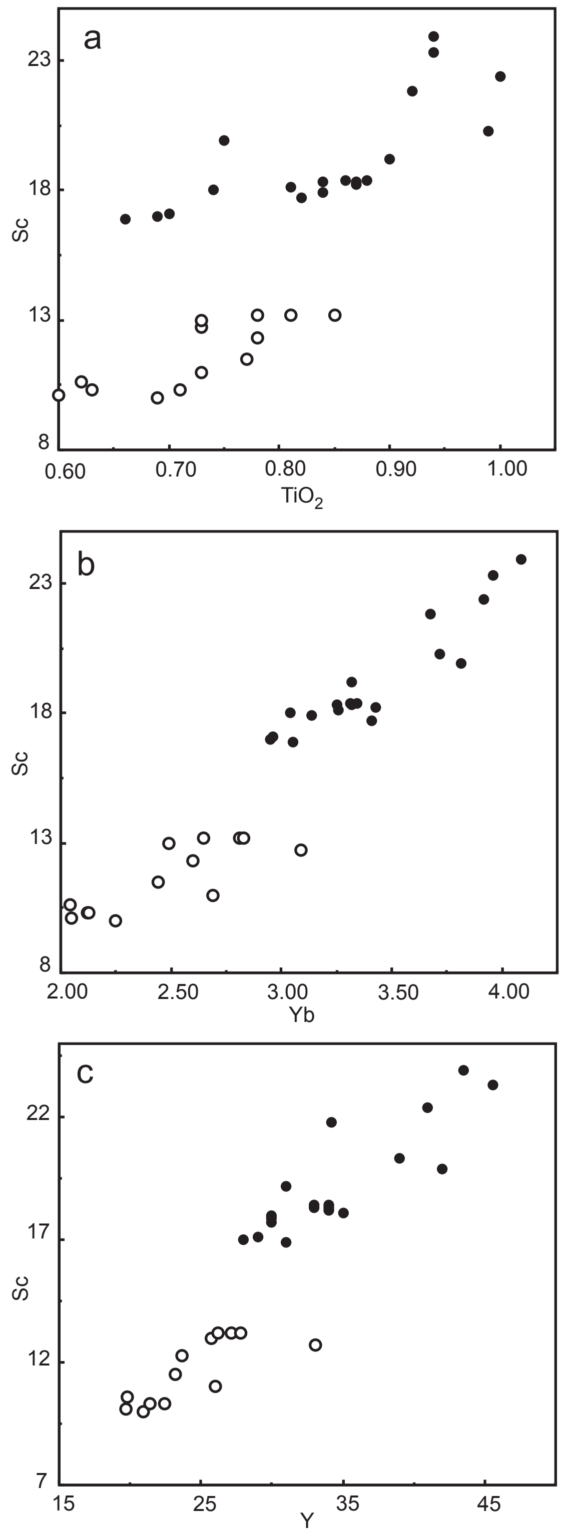

Supplementary Fig. 3: The covariations of SiO_2-Al_2O_3, SiO_2-K_2O andAl_2O_3-K_2O suggest that illiteAAl_2O_3l$_2$O$_3$ would be the main K-mineral in the underlying shales. Symbols as in Fig. 3.

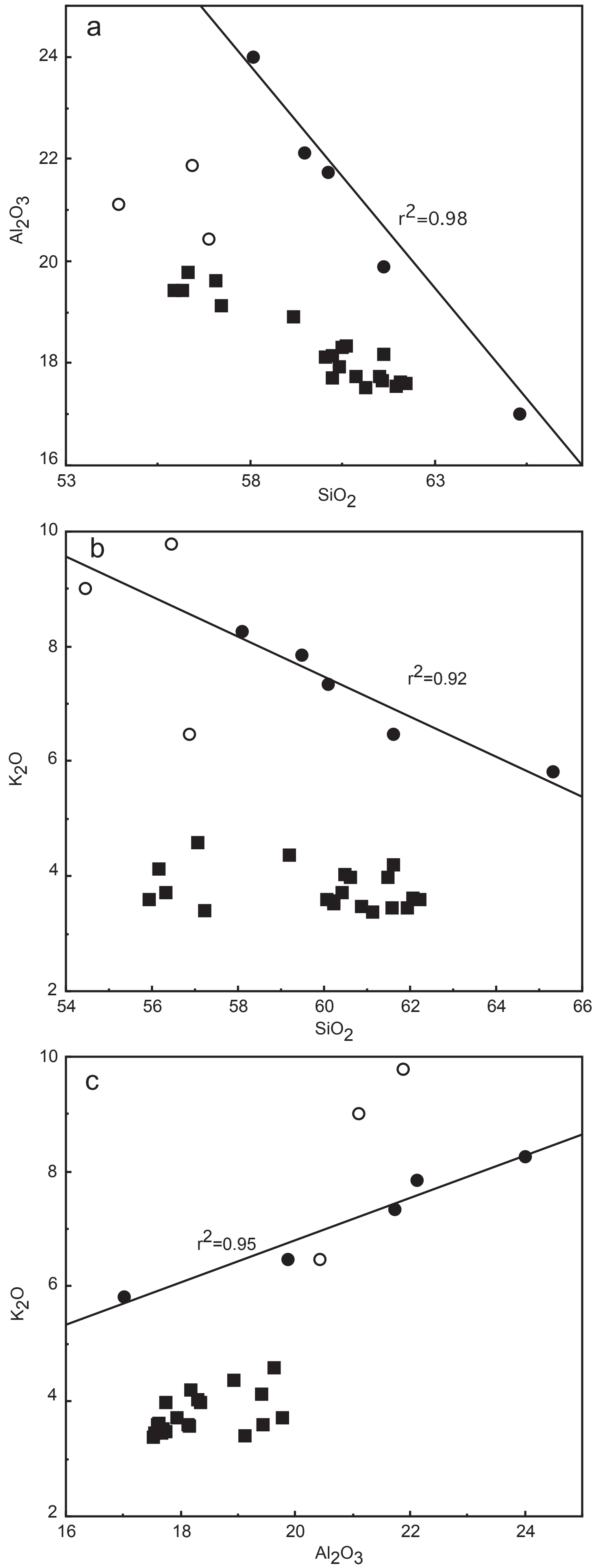

Supplementary Fig. 4. Chondrite-normalised REE patterns for the Lower Cambrian shales overlying (a) and underlying (b) the carbonate level. See text. Symbols as in Fig. 3.

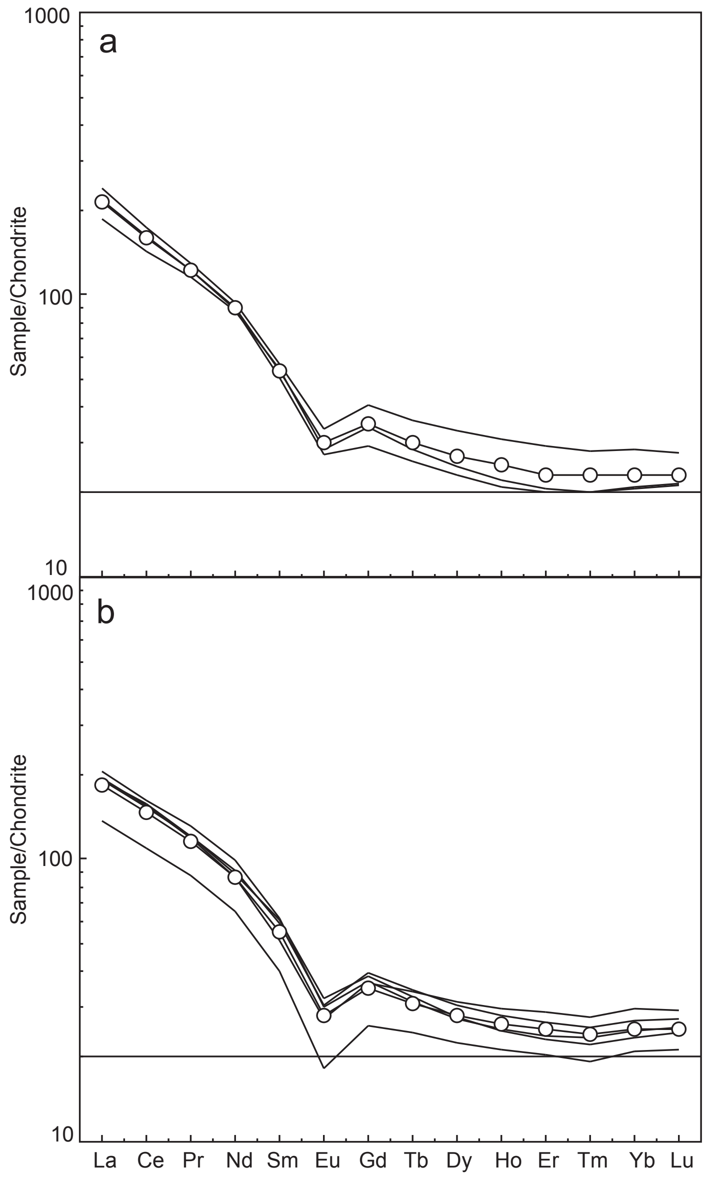

Supplementary Fig. 5: Diagrams TiO_2-P_2O5 and TiO_2-Zr for the Ediacaran shales. The positive covariations of these elements probably reflect similar proportions of Ti-minerals, phosphates and zircon in all samples. Symbols as in Fig. 3.

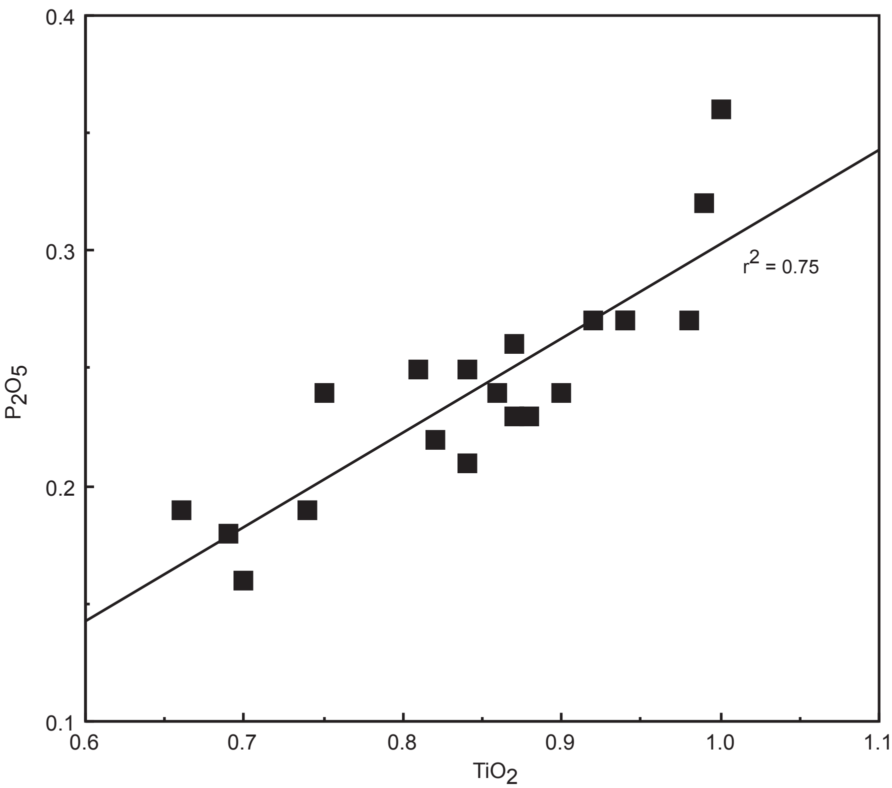

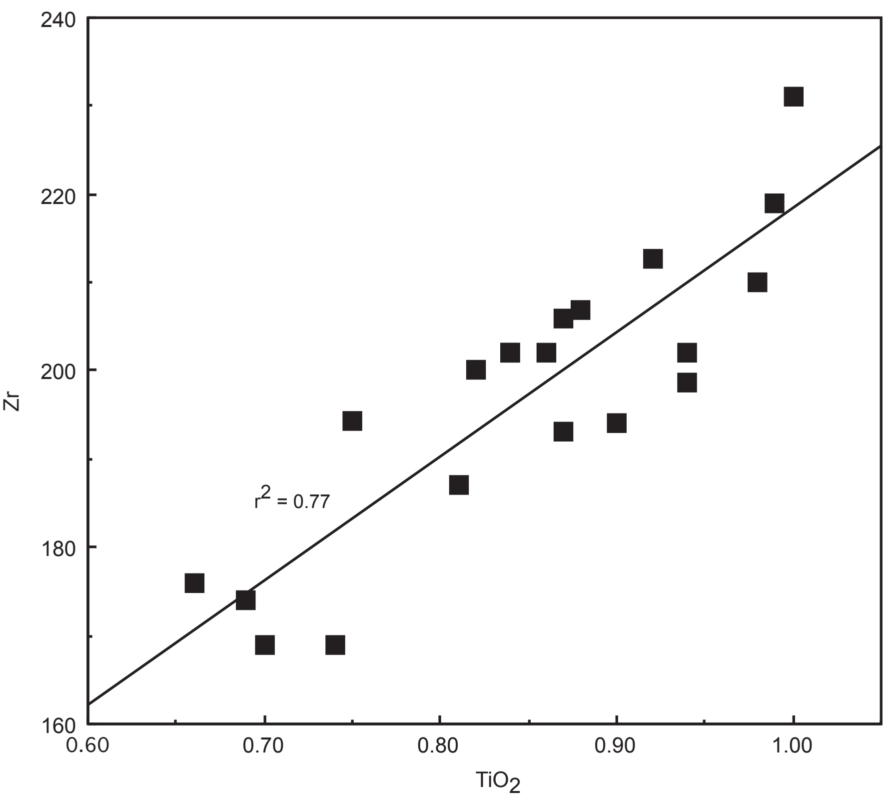

Supplementary references

Barbero, L., Villaseca, C., Rogers, G., Brown, P.E. 1995. Geochemical and isotopic disequilibrium in crustal melting: An insight from the anatectic granitoids from Toledo, Spain. *Journal of Geophysical Research*, **100**, 15745-15765.

Carignan, J., Hild, P., Mévelle, G., Morel, J. & Yeghicheyan, D. 2001. Routine analyses of trace elements in geological samples using flow injection and low pressure online liquid chromatography coupled to ICP-MS: a study of reference materials BR, DR-N, UB-N, AN-G and GH. *Geostandards Newsletters*, **25**, 187-198.

Pin, C. & Santos Zalduegui, J.F. 1997. Sequential separation of LREE, Th and U by miniaturized extraction chromatography: application to isotopic analyses of silicate rocks. *Analytica Chimica Acta*, **339**, 79-89.

Pourmand, A., Daupas, N. & Ireland, J.T. 2012. A novel extraction chromatography and MC-ICP-MS technique for rapid analysis of REE, Sc and Y: Revising CI-chondrite and Post-Archean Australian Shale. *Chemical Geology*, **291**, 38-54.

Schultz, L.G. 1964. Quantitative interpretation of mineralogical composition from X-Ray and chemical data for the Pierre Shale. *U.S. Geological Survey Professional Paper*, **391-C**, 1-31.

Thirlwall, M.F. 1991. Long-term reproductivility of multicollector Sr and Nd isotope ratio analysis. *Chemical Geology*, **94**, 85-104.

Wasserburg, G.J., Jacobsen, S.B., DePaolo, D.J., McCulloch, M.T. & Wen, T. 1981. Precise determination of Sm/Nd ratios, Sm and Nd isotopic abundances in standard solutions. *Geochimica et Cosmochimica Acta*, **45**, 2311-2323.